

# 1    **Maternal effects on early-life gut microbiome maturation in**

## 2    **a wild nonhuman primate**

3

4    Alice Baniel<sup>1,2</sup>, Lauren Petrullo<sup>3</sup>, Arianne Mercer<sup>4</sup>, Laurie Reitsema<sup>5</sup>, Sierra Sams<sup>4</sup>, Jacinta C.  
5    Beehner<sup>3,6</sup>, Thore J. Bergman<sup>3,7</sup>, Noah Snyder-Mackler<sup>1,2,8,†</sup>, Amy Lu<sup>9,†</sup>

6

## 7    **AFFILIATIONS**

8    <sup>1</sup> Center for Evolution and Medicine, Arizona State University, Tempe, AZ, 85281, USA

9    <sup>2</sup> School of Life Sciences, Arizona State University, Tempe, AZ, 85287, USA

10    <sup>3</sup> Department of Psychology, University of Michigan, Ann Arbor, MI 48109, USA

11    <sup>4</sup> Department of Psychology, University of Washington, Seattle, WA 98195, USA

12    <sup>5</sup> Department of Anthropology, University of Georgia, Athens, GA 30602, USA

13    <sup>6</sup> Department of Anthropology, University of Michigan, Ann Arbor, MI 48109, USA

14    <sup>7</sup> Department of Ecology and Evolutionary Biology, University of Michigan, Ann Arbor, MI 48109, USA

15    <sup>8</sup> School for Human Evolution and Social Change, Arizona State University, Tempe, AZ, 85287, USA

16    <sup>9</sup> Department of Anthropology, Stony Brook University, Stony Brook, NY, 11794, USA

17    <sup>†</sup>Amy Lu and Noah Snyder-Mackler contributed equally to this work.

18

## 19    **Corresponding authors:**

20    Alice Baniel (alice.baniel@gmail.com)

21    Amy Lu (amy.lu@stonybrook.edu)

22    Noah Snyder-Mackler (nsnyderm@asu.edu)

23 **ABSTRACT**

24 Early-life gut microbial colonization is an important process shaping host physiology, immunity  
25 and long-term health outcomes in humans and other animals. However, our understanding of this  
26 dynamic process remains poorly investigated in wild animals, where developmental mechanisms  
27 can be better understood within ecological and evolutionary relevant contexts. Using 16s rRNA  
28 amplicon sequencing on 525 fecal samples from a large cohort of infant and juvenile geladas  
29 (*Theropithecus gelada*), we characterized gut microbiome maturation during the first three years  
30 of life and assessed the role of maternal effects in shaping offspring microbiome assembly.  
31 Microbial diversity increased rapidly in the first months of life, followed by more gradual changes  
32 until weaning. As expected, changes in gut microbiome composition and function with increasing  
33 age reflected progressive dietary transitions: in early infancy when infants rely heavily on their  
34 mother's milk, microbes that facilitate milk glycans and lactose utilization dominated, while later  
35 in development as graminoids are progressively introduced into the diet, microbes that metabolize  
36 plant complex polysaccharides became dominant. Furthermore, the microbial community of  
37 nursing infants born to first-time (primiparous) mothers was more "milk-oriented" compared to  
38 similarly-aged infants born to experienced (multiparous) mothers. Comparisons of matched  
39 mother-offspring fecal samples to random dyads did not support vertical transmission as a conduit  
40 for these maternal effects, which instead could be explained by slower phenotypic development  
41 (and associated slower gut microbiome maturation) in infants born to first-time mothers. Together,  
42 our findings highlight the dynamic nature of gut colonization in early life and the role of maternal  
43 effects in modulating this trajectory in a wild primate.

## 44 INTRODUCTION

45 The colonization of the gastrointestinal tract begins at birth and develops into a trajectory that can  
46 be highly variable between individuals [1–8]. Variation in the source and timing of postnatal  
47 microbial colonization influences somatic growth [9–12], neuroendocrine [13,14] and immune  
48 physiology [15–17], with health and fitness consequences that can extend across the life course  
49 [16,18,19]. In humans, for instance, infants that take antibiotics during the first year of life are  
50 more likely to develop allergies, asthma, and inflammatory bowel disease during childhood [20–  
51 23]. Germ-free rodent models demonstrate that at least some of these effects are causally related  
52 to the microbiome and are long-lasting. For example, germ-free rodents develop structural  
53 abnormalities of the gastrointestinal tract [15,24] that translate into immune system dysfunction  
54 later in life [25,26], an outcome that can only be partly reversed by introducing microbes during  
55 critical periods of development [27,28]. Despite the critical role that early-life gut microbial  
56 colonization plays in host development, research thus far has mainly focused on clinical studies in  
57 humans [14,22,29–31], complemented by experimental studies on laboratory rodents [32–35] and  
58 domestic animals [9,36–39]. Studies of wild animals are needed if we want to understand host–  
59 microbiome coevolution within a broader ecological and evolutionary context and without the  
60 confounding factors associated with medical interventions (e.g., Cesarean section, antibiotic use,  
61 formula feeding) [17,40,41].

62 The maternal microbiota drives gut microbiome assembly in offspring via vertical  
63 transmission of a large number of microbial lineages [42–46]. Vertical transmission is thought to  
64 be particularly strong in mammals due to viviparity and extended periods of lactation and post-  
65 weaning maternal care [47]. The first important exposure to microbes occurs during birth, when  
66 infants are inoculated with maternal vaginal, fecal, and skin microbiota [3,5,8,29,44,48].

67 Postnatally, vertical transmission is primarily accomplished through nursing, with numerous  
68 microbes and milk glycans (i.e., oligosaccharides) transmitted through milk that, together,  
69 determine the microbial composition of the infant's gut [42,49,50]. While milk microbes directly  
70 seed the offspring's gut, milk glycans promote the growth of beneficial microbes, such as  
71 *Bifidobacterium* and *Bacteroides*, that in turn break the glycans down into forms usable by the host  
72 [51–53]. Although breastmilk is the most obvious route by which vertical transmission takes place  
73 [10,49,50,54], studies on humans suggest that the maternal gut microbiome is also a major source  
74 of transmitted strains [42,44,55,56]. Maternal gut microbes might be transmitted to offspring via  
75 milk, as the gastrointestinal tract is hypothesized to be the major reservoir of microbes colonizing  
76 the mammary gland (the enteromammary pathway) [49,57]. Alternatively or additionally, mothers  
77 may transmit gut microbes to offspring via preferential body contact [58], a mechanism that  
78 suggests vertical transmission can continue in some capacity past weaning [47]. Because maternal  
79 microbial taxa are the first to colonize and tend to be better adapted to the gut ecological niche  
80 compared to other environmental microbes, they often persist longer in offspring than those  
81 acquired from other sources [42,56,59].

82 Recent studies suggest that microbiome-mediated maternal effects are indeed possible. In  
83 several mammals, maternal traits, such as parity (i.e., the number of times a mother has given  
84 birth), have been associated with differences in the composition of both maternal [39,60] and  
85 offspring microbial communities [10,39]. In nonhuman primates (vervet monkeys: *Chlorocebus*  
86 *pygerythrus*), infants born to low-parity mothers harbored reduced microbial diversity and a  
87 greater abundance of *Bacteroides fragilis* [10], a bacterium derived from the milk microbiota that  
88 is specialized in digesting milk glycans [61,62]. In turn, infants from low-parity females grew  
89 faster, suggesting that low-parity mothers may compensate for poor milk production by vertically

90 transmitting milk microbes that could help infants extract more energy from lower milk volumes  
91 [10]. Such strategies may be broadly beneficial to dyads in which mothers cannot provide adequate  
92 nutritional resources to offspring (e.g., low-ranking mothers) [63,64]. Thus, maternal vertical  
93 transmission of microbes may be an important mechanism of phenotypic plasticity during lactation  
94 [64,65].

95 Primates are particularly relevant models for understanding postnatal microbiome  
96 development and maternal effects because they are closely related to humans, display prolonged  
97 lactation periods, and engage in high maternal investment [66,67]. Furthermore, maternal  
98 condition (e.g., energetic status) and maternal traits (e.g., dominance rank, social integration  
99 parity) are known to influence offspring developmental and long-term fitness outcomes [68–71].  
100 Although studies on host-associated microbial communities in wild primates are emerging, many  
101 remain limited in scope, hampered by cross-sectional samples and small sample sizes of unweaned  
102 infants (particularly in the first few weeks of life), which together prevent longitudinal  
103 characterization of gut microbial colonization processes [72–75]. Here, we used dense cross-  
104 sectional and longitudinal monitoring to characterize gut microbial colonization during the first  
105 three years of life and assess the role of maternal effects in shaping offspring maturation  
106 trajectories in wild gelada monkeys (*Theropithecus gelada*). Geladas live in the high-altitude  
107 plateaus of Ethiopia and have a specialized graminivorous diet (at times, comprising 90% grass)  
108 [76,77], which strongly shapes the composition and function of the adult gut microbiome [78,79].  
109 Because geladas live in polygynous reproductive units that range together in larger bands  
110 (comprised of 200 or more individuals) [80], we are able to monitor over 50 immatures at any  
111 given time, offering an unprecedented sample size to examine gut microbial characteristics during  
112 early life in a wild primate. We used 16s rRNA amplicon sequencing on 525 fecal samples from

113 89 immatures to profile changes in gut microbiome diversity, composition, and function during  
114 the first three years of life (N=5.9±5.5 samples per individual, range:1-18, **Figure S1**). In our  
115 population, geladas reach weaning at approximately 1.5 years of age and become sexually mature  
116 around 4.6 years [81]; and maternal characteristics, such as parity and dominance rank, are known  
117 to influence inter-individual variation at both of these developmental milestones [Feder et al., in  
118 revision; Lu et al., unpublished]. We predicted that early life microbial changes would reflect  
119 dietary transitions associated with weaning, as infants transition from milk to a plant-based diet  
120 [5,48,82,83]. We also predicted that maternal traits, such as dominance rank and parity would be  
121 associated with inter-individual differences in gut microbiome diversity, composition, and  
122 function in offspring. More specifically, we predicted that infants born to primiparous and low-  
123 ranking mothers would have a microbiome more functionally adapted to digest milk to compensate  
124 for poorer maternal energetic allocation during lactation. Lastly, we tested if we could detect  
125 evidence of vertical transmission between mother and offspring using fecal-fecal comparisons of  
126 mother-infant dyads (with 398 matched fecal samples between mother and offspring collected on  
127 the same day throughout development) and if greater vertical transmission in certain females (e.g.,  
128 low rank, first-time mothers) could be the conduit for putative maternal effects on offspring's  
129 microbiome composition. We expected a stronger signal of vertical transmission in early life  
130 [10,42,44,55,56], likely driven by a combination of greater microbial transfer via milk when  
131 infants are nursing and are also in more frequent body contact with their mother.

132

## 133 **RESULTS**

### 134 ***General pattern of gut microbiome maturation in geladas***

135 We characterized the gut microbiome across 525 immature gut microbiome samples, and detected  
136 3,784 Amplicon Sequence Variants (ASVs) (mean±SD per sample: 728±261, min-max: 65-1,498)

137 belonging to 19 phyla and 76 families. The gut microbiome composition of immature geladas  
138 changed quickly following birth, with an initial phase of taxonomic succession and diversification  
139 during the first few months of life, followed by a progressive stabilization of the overall community  
140 (**Figures 1A,B**).

141 To characterize broad changes in gut microbial community composition across  
142 development, we first focused on patterns of alpha diversity (i.e., the microbial diversity within a  
143 sample) and beta diversity (i.e., the overall difference of composition between samples). The  
144 Shannon Index of alpha diversity was initially low in early life and increased rapidly with age  
145 (GAMM:  $edf=7.2$ ,  $P<2.0\times 10^{-16}$ ) (**Figure 1C, Table S1**), converging to adult-like values at 7.3  
146 months (nonlinear quadratic plateau model:  $R^2=0.62$ ) (see **Figure S2, Table S1** for similar results  
147 on alternative alpha diversity metrics). Furthermore, age was one of the strongest predictors of the  
148 difference in microbial composition between samples (PERMANOVA based on Aitchison  
149 dissimilarity metric of beta diversity:  $R^2=0.75$ ,  $P<9.9\times 10^{-5}$ , **Table S2, Figures 1D,E**) and samples  
150 clustered tightly by age on the first axis (PC1) of a Principal component analysis of beta diversity  
151 (Pearson correlation coefficient between age and PC1=0.62,  $P<2.2\times 10^{-16}$ ). Compared to alpha  
152 diversity, beta diversity reached an adult-like composition later in development, at 17.2 months  
153 (nonlinear quadratic plateau model between PC1 and age:  $R^2=0.55$ ; **Figure 1D**), which is  
154 approximately the age at which gelada mothers return from lactational amenorrhea and resume  
155 reproductive cycles [81]. Other important structuring factors of the immature gut microbiome  
156 included infant identity ( $R^2=0.24$ ) and group membership ( $R^2=0.05$ ) (**Table S2**).

157 To assess the compositional maturation of the gut microbiome of immature geladas relative  
158 to the maternal gut microbiome across age, we calculated the number of shared ASVs and beta  
159 diversity dissimilarity (unweighted and weighted UniFrac) between 398 matched immature-

160 mother pairs of fecal samples collected the same day. As offspring got older, they shared an  
161 increasing number of bacteria with their mother (GAMM: effective degree of freedom, edf=4.7,  
162  $P<2.0\times10^{-16}$ ; **Table S3, Figure 1F**) and became more similar to maternal (i.e., adult-like) gut  
163 microbiome composition (unweighted UniFrac: edf=4.7,  $P<2.0\times10^{-16}$ ; weighted UniFrac: edf=3.5,  
164  $P<2.0\times10^{-16}$ ; **Table S3, Figure S3**). Convergence with maternal gut occurred at 14.5 months for  
165 the number of shared ASVs (nonlinear quadratic plateau model:  $R^2=0.44$ ; **Figure 1F**) and 14.8-  
166 15.5 months for beta diversity dissimilarity ( $R^2=0.48$  for unweighted UniFrac and  $R^2=0.17$  for  
167 weighted UniFrac; **Figure S3**).

168 Despite the strong age-related patterns noted above, inter-individual variability in  
169 composition (as measured by the minimal pairwise beta diversity dissimilarity value among  
170 immature samples, see Methods) was higher among younger infants compared to older juveniles  
171 (**Figure 1G**). Some young infants (~3-6 months) in particular had a gut microbiome that were  
172 relatively mature (i.e. adult-like) for their age (**Figure 1D**). Such “individuality” in the gut  
173 microbiome in early life was likely driven by the presence of rare taxa, since the pattern was  
174 stronger using unweighted UniFrac (which does not take into account taxa abundance) as opposed  
175 to weighted UniFrac measures of beta diversity (**Figure 1G**).

176

### 177 ***Taxonomic and functional changes during development***

178 To characterize age-associated changes in microbial composition and function, we used  
179 autoregressive integrated moving average (ARIMA) models to identify significant developmental  
180 changes in the abundance of each microbial taxa (at the family and genus levels) and each predicted  
181 functional pathway (at the metabolic level: KEGG Orthologs, KOs and enzymatic level: Enzyme  
182 Commission numbers, EC [84]). We then used hierarchical clustering to group microbial taxa and

183 functional pathways based on similar age-related abundance trajectories. Maturational trajectories  
184 fell into one of four distinct clusters at both the taxonomic (**Figure 2, S4; Table S4**) and functional  
185 (KOs: **Figure S5-S6, Table S5**; EC: **Figure S7, Table S6**) levels.

186

187 **Cluster 1: The early-life microbiome is adapted to process milk**

188 Cluster 1 contained microbes that were abundant during the earliest months of infancy (18  
189 families: **Figure 2A, Table S4** and 39 genera: **Figure S4, Table S4**) and are broadly involved in  
190 using and fermenting milk sugars (see supplemental results 1 for additional details on cluster 1).  
191 These early colonizers comprised bacteria that break down milk glycans (Bacteroidaceae,  
192 Bifidobacteriaceae) and lactose (Streptococcaceae, *[Ruminococcus] gnavus* group) and other  
193 groups that ferment glycans and lactose into butyrate (Lachnospiraceae: *Lachnoclostridium*,  
194 *Blautia*, *Anaerostipes*, and Ruminococcaceae: *Faecalibacterium*, *Butyricicoccus*, *Butyricimonas*)  
195 or propionate (Veillonellaceae) (**Figures 2B and 3A**). *Bacteroides* appeared to be the main  
196 degrader of milk glycans in geladas, representing the most abundant genus in early life (~30% of  
197 the gut microbes at 1 month) (**Figure 3A**). One *Bacteroides* ASV – *B. fragilis*, a proficient  
198 degrader of milk glycans [61] – was particularly abundant in early life (i.e., with a high loading  
199 score on PC1, **Table S7**). By contrast, *Bifidobacterium* – an important milk glycan degrader in  
200 humans – was present at extremely low abundance across development (<0.01% at 1 month in  
201 geladas vs ~40% in humans [85]) (**Figure 3A**).

202 Functional cluster 1 also reflected the involvement of the gut microbiome in milk  
203 utilization and immunity pathways (metabolic cluster 1: **Figures S5-S6, Tables S5** and enzymatic  
204 cluster 1: **Figure S7, Table S6**). Young infant gut microbiomes contained high levels of bacterial  
205 genes involved in carbohydrate metabolism, notably in the catabolism of fructose, mannose, and  
206 galactose (3 abundant milk sugars [86]), and in the conversion of sugars to energy (e.g., via

207 glycolysis/gluconeogenesis, pyruvate metabolism, pentose phosphate pathway) (**Figure 4A**).  
208 Similar functional signatures of cluster 1 were also apparent at the enzymatic level, as the gut  
209 microbes encoded a specialized enzymatic toolkit (alpha and beta glucosidase, alpha and beta  
210 galactosidase, fucosidase, sialidase, beta-hexosaminidase) necessary to cleave complex milk  
211 glycans (**Figure S8, Table S6**). *Bacteroides* was the main microbial group encoding those  
212 enzymes (**Figure S8**), confirming its central role in milk glycan degradation in geladas.

213 Interestingly, cluster 1 also included several putatively pathogenic genera (**Figure 3B**),  
214 including some bacterial species most responsible for enteric infections and diarrheal diseases in  
215 human newborns and captive animals (e.g., *Clostridioides difficile*, *Helicobacter macacae*,  
216 *Clostridium butyricum*, *C. perfringens* [87–91]) (**Table S7**). It also included 3 major groups of  
217 mucin-degrading bacteria (*Akkermansia*, [*Ruminococcus*] *gnavus* group and [*Ruminococcus*]  
218 *torques*) (**Figure 3C**) that are involved in the development of the intestinal mucosa, a primary line  
219 of immune defense [92]. These taxa reflect the importance of the developing immune system at  
220 this stage in life. In line with this interpretation, the early life microbial metabolic pathways tended  
221 to be more involved in processes related to the host immune system (e.g NOD-like receptor) and  
222 nervous system (e.g., glutamatergic synapse pathway) (**Figure 4A, Tables S5**).

223

224 **Clusters 2 & 3: The weaning transition is accompanied by important gut microbial**  
225 **rearrangements**

226 Around 10 months of age, a small number of microbial taxa (**Figures 2A and S4, Tables S4**) and  
227 metabolic pathways (**Figures S5-S6, Tables S5**) peak (cluster 2) or decrease (cluster 3) in  
228 abundance. Of these changes, the most notable included peaks in Lactobacillaceae (genus  
229 *Lactobacillus*), Prevotellaceae, and Lachnospiraceae (cluster 2, **Figure 2C**). While  
230 Lactobacillaceae is a keystone lactic acid bacterial group producing large amounts of lactate from

231 milk sugars, Prevotellaceae and Lachnospiraceae (**Figure 2C**) are fiber-degrading genera. These  
232 transient shifts highlight the role of the gut microbiome in digesting both milk and plant items at  
233 this age.

234 Taxonomic changes at ten months translated at the functional level into a remodeling of  
235 the metabolism of amino acids, with an increase in microbial genes involved in alanine, aspartate,  
236 glutamate, cysteine, and methionine metabolism (cluster 2), and a decrease in microbial genes  
237 involved in phenylalanine (found in breast milk), glutathione (antioxidant typically enriched in the  
238 first weeks of life in humans), and tyrosine metabolism (cluster 3) (**Figure 4B, Tables S5**).  
239 Microbial genes involved in sporulation and germination were also more highly expressed (**Figure**  
240 **4B, Table S5**), suggesting some changes in persistence strategy from the spore-forming microbes  
241 in the gut.

242

#### 243 **Cluster 4: The later-life gut microbiome is adapted to a plant-based diet**

244 Cluster 4 was characterized by 22 families (**Figure 2A, Table S4**) and 63 genera (**Figure S4,**  
245 **Table S4**) that increased sharply with age and plateaued in older immatures (from 10 months of  
246 age onward), including cellulolytic (Spirochaetaceae, Fibrobacteraceae, *Cellulosilyticum*) and  
247 fermentative taxa (Lachnospiraceae, Clostridiales Family XIII, several genera from Prevotellaceae  
248 and Ruminococcaceae), as well as RFP12 (**Figure 2D**), which are all commonly found in adult  
249 geladas [79]. These taxa are involved in metabolizing complex plant polysaccharides found in  
250 graminoid leaves and roots, which comprise the majority of the adult gelada diet.

251 At the functional level (cluster 4, **Figures S5-S6, Tables S5**), the gut of old immatures  
252 harbored more bacterial genes involved in energy, amino acid, and lipid metabolism and in the  
253 regulation of genetic expression and bacteria growth (nucleotide metabolism, replication and

254 repair, genetic information processing and translation) (**Figure 4C**), a functional profile that is  
255 typical of the adult gelada gut [79].

256

257 ***Maternal effects on offspring gut microbiome composition and function***

258 We next examined whether inter-individual variability in gut microbiome composition early in life  
259 (**Figure 1D,G**) could be explained, in part, by maternal traits, including maternal dominance rank  
260 and parity. We ran these analyses using (i) all samples (0-3 years, N=525), but since we predicted  
261 that maternal effects on the offspring microbiome would be strongest in early life (when infants  
262 are still nursing), we also ran separate analyses only focusing on (ii) young infants (<12 months of  
263 age, still relying largely on milk, N=184) and (iii) old immatures (>18 months, relying largely on  
264 plants, N=259). Note that we ran separate analyses for each age group because it is not possible to  
265 fit an interaction between a smooth term (i.e., age) and covariates (i.e., maternal attributes) in  
266 GAMMs.

267 Maternal dominance rank did not influence the alpha or beta diversity (**Tables S1-S2**,  
268 **Figure S9**) of immature gut microbiomes, nor did it predict differences in microbial families,  
269 genera, or functional pathways (**Tables S8-S10** for (ii) young infants, results not shown for (i) all  
270 immatures or for (iii) old immatures). Maternal parity also did not exert a significant influence on  
271 the diversity, composition, or relative abundance of taxa in the immature gut microbiome (**Tables**  
272 **S1, S2, S8**). However, parity was significantly associated with the relative abundance of several  
273 microbial metabolic pathways (**Table S9**) and enzymes (**Table S10**) during the first 12 months of  
274 life (results non-significant for (i) all immatures or (iii) old immatures). Namely, infants born to  
275 primiparous females had functional profiles more typical of early life (<12 months) and related to  
276 milk digestion, both at the metabolic and enzymatic levels. Their gut microbes were more involved

277 in carbohydrate metabolism (e.g., galactose, fructose and mannose metabolism), cellular processes  
278 and signaling, and nervous system function (**Figure 5A**); and they harbored a higher abundance  
279 of key enzymes that cleave milk glycans (**Figure S10**). By contrast, young infants (<12 months)  
280 born to multiparous females had a more functionally “mature” gut microbiome for their age, with  
281 higher abundance of later-life microbial pathways such as amino acid metabolism and nucleotide  
282 metabolism (**Figure 5B**). To determine why maternal parity had an effect at the functional level  
283 but not at the taxonomic level, we examined the bacterial taxa that showed a statistical trend to be  
284 more abundant in young infants (<12 months) born to primiparous females (i.e., with p-values<0.1  
285 before FDR correction, **Table S9**). Offspring of primiparous mothers indeed tended to harbor a  
286 higher abundance of microbial taxa involved in milk digestion (e.g., Lachnospiraceae,  
287 Bacteroidaceae, Clostridiaceae 1) (**Figure S11**, see supplemental results 2), which suggests that  
288 individual taxa exert small additive effects that were only detected at the functional level.  
289

#### 290 ***Mother-to-infant vertical transmission***

291 Previous work on captive primates suggests that the effect of maternal parity on microbial function  
292 could be mediated by differences in vertical transmission between multi- and primiparous females,  
293 with primiparous females transferring more milk-oriented microbes to their offspring (via the  
294 milk) [10]. We tested if we could statistically detect evidence of vertical transmission between  
295 mother and offspring using fecal-fecal microbiome comparisons. We used a nonparametric  
296 resampling approach to test if mother-offspring pairs of fecal samples were more similar than  
297 expected by chance (i.e compared to when we match the immature sample with random adult  
298 female samples), as measured by the number of shared ASVs or beta dissimilarity. We predicted  
299 that vertical transmission would be strongest in early life (when infants are still nursing), thus we  
300 ran analyses using either (i) all samples (0-3 years, N=398 pairs) or focusing on (ii) young infants

301 (<12 months of age, N=136 pairs) and (iii) old immatures (>18 months of age, N=201 pairs)  
302 separately. Using all pairs, we found that immatures shared 3.4% more ASVs (observed  
303 value=355, random value=343,  $P<1.0\times10^{-3}$ ) and were 1.8% more similar compositionally  
304 (unweighted UniFrac dissimilarity: observed=0.55, random=0.56,  $P=1.0\times10^{-3}$ ) to their own  
305 mother than with random adult females of the population (**Table S11**), potentially indicative of  
306 vertical transmission. However, unexpectedly, this signal was weaker and non-significant in the  
307 youngest infants (0-12 months: number of shared ASVs: observed=251, random=245,  $P=0.09$  and  
308 unweighted UniFrac dissimilarity: observed=0.67, random=0.67,  $P=0.26$ ; **Figures 5C and S12**,  
309 **Table S11**), and was strongest and significant in older juveniles (>18 months: number of shared  
310 ASVs: observed=412, random=398,  $P=2.0\times10^{-3}$  and unweighted UniFrac dissimilarity: observed  
311 value=0.49, random value=0.50,  $P=1.0\times10^{-3}$ ; **Figures 5C and S12, Table S11**). The finding of  
312 greater vertical transmission after, rather than before, nursing cessation suggests that these mother-  
313 offspring similarities were mostly mediated by non-nursing interactions and that milk vertical  
314 transmission may not be adequately captured by comparing infant and maternal fecal microbiomes.

315 Moreover, the ASVs shared between mother-infant pairs in the first 12 months of life were  
316 not the same ASVs found abundant in early-life (i.e., ASVs with a negative score on PC1) and  
317 therefore not related to nursing (**Figure 5D, Table S12**). For example, *Bacteroides fragilis* is found  
318 in 49% of infants <12 months but is only shared in 9% of mother-infant pairs. Instead, the most  
319 commonly shared ASVs among mother-infant pairs between 0-12 months tended to be ASVs  
320 characterizing later life (i.e., with positive scores on PC1), characteristic of older offspring and of  
321 adult females (**Figure 5D, Table S12**). Thus, mother-infant pairs share more bacteria and have  
322 more similar gut microbial community than expected by chance, but this shared community

323 belongs to the typical adult microbiome of geladas, and is not specific to microbes functionally  
324 beneficial to processing milk during the early developmental period.

325 Since infants of primiparous females possessed more milk-oriented microbes (i.e., far from  
326 adult-like microbes), we also found that they shared fewer ASVs ( $\beta=-74.5, P=0.01$ ) and were more  
327 dissimilar to their mother (unweighted UniFrac:  $\beta=0.07, P=0.03$ ) in the first 12 months of life than  
328 infants born to multiparous females (**Figure 5E, Table S3**). However, this effect of greater  
329 dissimilarity in primiparous-infant dyads disappeared later in life (>18 months of age) when the  
330 effect of maternal parity was no longer detected (number of shared ASVs:  $\beta=11.0, P=0.46$ ,  
331 unweighted UniFrac:  $\beta=-3.5 \times 10^{-3}, P=0.81$ ) (**Figure 5E, Table S3**). This result shows that the  
332 effect of maternal parity on the offspring gut microbiome in the first 12 months of life is not  
333 mediated by stronger vertical transmission of milk-oriented microbes when using fecal-fecal  
334 comparisons.

335

## 336 **DISCUSSION**

337 We provide a detailed description of the compositional assemblage and functional development of  
338 the infant gut microbiome in a nonhuman primate during the first three years of life. As expected,  
339 age was the strongest structuring factor of the diversity, composition, and function of the gut  
340 microbiome. Most microbial taxa had clear age-related trajectories and could be grouped into four  
341 main clusters that reflected progressive dietary transitions associated with weaning. In addition,  
342 our data show that maternal effects were an important factor modulating offspring gut microbiome  
343 both during nursing and after weaning.

344 The broad dynamic of microbial colonization in geladas presents many similarities with  
345 previous reports on humans [2,5,8] and other mammals ([10,37,73], but see[74]). We observed a

346 low initial number of microbes and a rapid increase in microbial diversity in the first seven months  
347 of life, followed by more gradual changes in microbial composition until weaning (~17 months).  
348 The fact that maximal microbial diversity was attained by the time infants reached 7 months, while  
349 the microbial community continued to evolve until weaning, suggests that numerous events of  
350 lineage extinction and *de novo* colonization continue to take place in the gelada gut until weaning.  
351 Similar to humans [5,42,93], it is the cessation of nursing rather than just the introduction of solid  
352 foods (which usually starts as early as the first few weeks after birth in geladas) that really drives  
353 the maturation of the developing gut microbiome to an adult-like composition. Indeed, weaning  
354 marks two important transitions that can have dramatic effects on the maturing gut microbiome.  
355 First, as milk is replaced by solid foods, the nutrient sources for host and microbes both change,  
356 altering the types of microbes that are likely to flourish. Second, weaning is accompanied by the  
357 loss of maternal-origin immunologic factors and milk-derived microbes [94], both of which can  
358 further alter the microbiome through processes of selective seeding. Shifts in gut microbiome  
359 composition and function closely followed progressive dietary transitions: gut bacteria that  
360 facilitate milk glycans and lactose utilization were dominant in the gelada microbiome during early  
361 infancy, while cellulolytic and fibrolytic bacteria that metabolize plant complex polysaccharides  
362 were dominant later in development as graminoids were progressively introduced in the diet [76].  
363 Many of the early life colonizers were similar to those found in humans, such as *Bacteroides*,  
364 *Streptococcus*, *Faecalibacterium*, Lachnospiraceae, *Blautia*, *Clostridium*, *Veillonaea*, *Escherichia*-  
365 *Shigella*, and Pasteurellaceae [48,82,95] which perhaps suggest a set of universal mammalian or  
366 primate infant microbial taxa. These early-life microbes work as a metabolic network that relies  
367 on cross-feeding between primary degraders (e.g., lactose-degraders such as *Streptococcus*) and  
368 secondary fermenters (e.g., lactate-utilizers such as *Veillonaea*) to convert milk sugars into energy

369 [96]. The functional enrichment in carbohydrate metabolism and fermentative pathways found in  
370 gelada infants is also typically observed in human newborns [2,5,55,97].

371 *Bacteroides*, and in particular *B. fragilis* [61,98], appear to be the primary microbial taxa  
372 involved in milk glycan degradation in geladas, as evidenced by their high abundance in early-life  
373 and the fact that they encode the enzymatic toolkits necessary to cleave complex milk glycans  
374 (e.g., fucosidase, sialidase, beta-galactosidase). These bacterial enzymes are critical for host  
375 nutrition, as mammalian hosts are unable to produce them and therefore cannot utilize milk glycans  
376 independently of gut bacteria [82]. In humans, this function is largely met by *Bifidobacterium*, a  
377 taxa commonly found in high abundance in breastfed humans that also breaks down milk glycans  
378 [8,48,99,100]; however this taxon was almost entirely absent in young geladas. In fact, variation  
379 in the dominance of *Bifidobacterium* and *Bacteroides* appears the norm at both the species and  
380 population level: several studies in mammals [10,37,72,101] and in some human populations  
381 [3,85,95,97,102] have noticed the absence of *Bifidobacterium* but abundance of *Bacteroides* in  
382 most or at least some nursing infants. *Bifidobacterium* and *Bacteroides* have different glycan-use  
383 profiles [61,62,97] linked to species and population differences in milk composition, particularly  
384 the structure and the relative abundance of different milk glycans [103–105].

385 The early-life microbiome of geladas was also characterized by a high number of  
386 potentially pathogenic bacteria known to cause enteric infection in human newborns and captive  
387 animals (*Clostridioides*, *Helicobacter*, *Clostridium*) [87–91] and several bacterial groups involved  
388 in the activation of the host immune system such as butyrate-producing (*Blautia*,  
389 *Faecalibacterium*, *Butyrivibacter*, *Butyrivibronas*) and mucin-degrading bacteria (*Akkermansia*,  
390 *Ruminococcus gnavus* and *R. torques*). Collectively, this microbial profile suggests that immune  
391 function is a priority for gelada infants. Butyrate plays a key role in the maintenance of gut integrity

392 [106,107] and protection against enteric infection [108]. This microbial metabolite is also an  
393 important immunoregulator via its action on intestinal macrophages [109,110]. Mucolytic bacteria  
394 play an essential role in mucus turnover [111] and contribute to an essential immune barrier  
395 protecting the underlying epithelium from luminal pathogens [111] and are thus strongly involved  
396 in immunity in early life. *Bacteroides* are also likely involved in regulation of intestinal immunity  
397 in early life [112,113]. *Bacteroides fragilis* in particular is directly involved in the maturation of  
398 the immune system by directing the production of regulatory T cells and ensuring a balance  
399 between Th1 and Th2 immunologic response [114–117]. Functional analyses revealed that the gut  
400 microbes were more strongly involved in host immunity during the nursing period, highlighting  
401 that microbial colonization plays an important role in priming of the host immune system in  
402 geladas.

403 We detected important compositional and functional signatures of microbial rearrangement  
404 around 10 months of age (i.e., 5-7 months before nursing cessation). *Bacteroides* decrease  
405 substantially in the gelada gut microbiome, while two other taxa, *Lactobacillus* and *Prevotella*,  
406 increase in abundance. *Lactobacillus* is a lactic acid bacterium that consumes lactose [118,119].  
407 Its rise in abundance around the weaning transition indicates an increase in lactose availability in  
408 the colon, likely due to the loss of endogenous lactase of infants in the upper gut [120]. *Prevotella*  
409 is a keystone fiber-degrading bacterium typically enriched in individuals with a plant-based diet.  
410 In two other mammalian species (vervet monkeys: [10] and northern elephant seals (*Mirounga*  
411 *angustirostris*): [72]), *Prevotella* also increased in abundance during the weaning transition. The  
412 abundance of *Bacteroides* and *Prevotella* are generally inversely correlated in the gut, due to the  
413 trade-off between saccharolytic and proteolytic fermentation [121]. Thus, the growth of *Prevotella*  
414 closer to weaning might be related to the decrease in milk degrading bacteria (i.e., *Bacteroides*)

415 and could be a good indicator of the transition from milk to solid food consumption in mammals  
416 [10]. These taxonomic changes were also accompanied by important functional changes in the  
417 metabolism of amino acids, vitamins, and cofactors, setting up the microbial activity characteristic  
418 of the adult gut.

419 Finally, our results highlight that early-life gut microbiome composition and functionality  
420 can be influenced by maternal effects, both during the nursing period, but also after weaning.  
421 During the first 12 months of life, we found that infants of primiparous mothers harbored more  
422 bacteria that were functionally relevant for processing milk sugars, which parallel recent findings  
423 in vervet monkeys [10]. The authors in that study hypothesized that infants of primiparous mothers  
424 may compensate for poor maternal investment by seeding more milk-oriented microbes that help  
425 infants extract more energy from milk [10]. In support of this, *B fragilis* was more abundant in the  
426 milk of low-parity vervet females, which resulted in higher abundance of milk-oriented microbes  
427 in the infant gut, which in turn promoted faster growth in low-parity infants [10]. In our study,  
428 vertical transmission – as assessed by fecal-fecal comparison of maternal and offspring  
429 communities – was not identified as the mechanism generating such a parity effect. First, we did  
430 not find evidence of vertical transmission in the first 12 months of life (infants and mothers did  
431 not share more ASVs than expected by chance during nursing). Second, the microbes that *were*  
432 shared by mother-offspring pairs were associated with processing grass rather than early life  
433 functions such as processing milk glycans or sugars. Third, infants from primiparous females  
434 actually shared fewer microbes with their mother than infants from multiparous females (since the  
435 detected shared microbes are later-life microbes). This result suggests that vertical transmission of  
436 early colonizers/milk-oriented microbes might be more strongly mediated by the direct transfer of  
437 milk microbiota in geladas [10,49,50,54] and, in contrast to reports in humans [42,44,55,56], not

438 easily detected using fecal-fecal comparisons between infants and their mothers. In vervets, for  
439 instance, infants aged 2-5 days shared more bacterial strains with their mother's milk than with  
440 their mother's gut [10]. This parity effect could nonetheless result from host filtering processes  
441 coming from the offspring themselves [56]. Maternal microbiomes might be similar across parity  
442 status, but offspring of primiparous females might preferentially seed milk-oriented microbes from  
443 milk in response to poorer maternal energetic allocation. In the absence of milk samples, evidence  
444 for such mechanisms remains unclear in geladas.

445 Alternatively, the effect of maternal parity could reflect a faster pace of gut microbiome  
446 maturation for offspring born to multiparous mothers. The pattern of vertical transmission might  
447 be similar between primiparous and multiparous females, but offspring of multiparous females  
448 might share more microbes with their mother during the first 12 months of life because they are  
449 more mature for age (and because we only capture vertical transmission of grass-processing  
450 microbes). This interpretation is supported by the evidence that multiparous mothers wean their  
451 offspring about 5 months earlier than primiparous females in geladas (in our studied cohort and in  
452 absence of takeover: multiparous=17.1 months, primiparous=21.9 months). The greater similarity  
453 between multiparous mothers and their infants is thus more likely to be generated by accelerated  
454 gut microbiome development, suggesting that these infants are undergoing the weaning transition  
455 at a faster pace than their peers. Infants from multiparous females could be eating solid grass,  
456 gaining physical independence, and becoming socially integrated earlier than their peers, all  
457 of which could explain greater microbial resemblance to mothers (and other adults). Behavioral  
458 and development data, such as infant growth, are needed to investigate this hypothesis of  
459 accelerated development and their consequences on offspring phenotype.

460 Somewhat surprisingly, we did find that immature gut microbiomes were more similar to  
461 maternal gut microbiomes than expected by chance after weaning regardless of the parity status of  
462 the mother. Such an effect has been previously documented in wild red squirrels (*Tamiasciurus*  
463 *hudsonicus*) [122] and chimpanzees (*Pan troglodytes*) ([74] but see [123]). Host genetics, or  
464 socially transmitted microbes, may facilitate maternal-offspring gut microbiome similarities  
465 beyond the early postnatal period [47]. A recent study in yellow baboons (*Papio cynocephalus*)  
466 found that the gut microbiome, including both abundant and rare taxa, is highly heritable [124]  
467 suggesting that the convergence of the gut microbiota between mother and offspring in geladas  
468 could be due shared genes. Alternatively, or additionally, the higher similarity in later life could  
469 be generated by high frequency of social contacts between mothers and offspring that extend past  
470 weaning. Primate mothers and offspring form preferential social bonds long after weaning,  
471 relationships that are characterized by a high degree of proximity, physical contact and grooming,  
472 and are likely to represent an enduring source of maternal microbial inoculation for offspring  
473 [58,125]. Further work is needed to understand the relative importance of these mechanisms in  
474 explaining mother-infant similarity during juvenility.

475

476 *Conclusion*

477 Our results highlight that early-life gut microbiome composition and function can be influenced  
478 by maternal effects, both during nursing as well as after weaning. Maternal parity in particular was  
479 associated with the functional maturation of the microbiome in offspring, likely reflecting faster  
480 developmental pace of infants born to reproductively experienced mothers. As infants age and are  
481 weaned, they converge toward an adult-like gut microbiome that is more similar to the maternal  
482 gut microbiome than expected by chance. The long-term consequences of such microbially-

483 mediated maternal effects remain unknown but could potentially influence phenotypic outcomes  
484 such as growth and immune function. Our work also emphasizes that early life vertical  
485 transmission, mediated in large part by milk transfer, may not be detected using fecal-fecal  
486 comparisons of maternal and infant communities and would ideally require data on the milk  
487 microbiome whenever possible.

488

## 489 MATERIAL & METHODS

### 490 *Study population and study site*

491 The data for this study were collected between Jan 2015 and Jan 2019 from a population of wild  
492 geladas living in the Simien Mountains National Park in northern Ethiopia (13°15'N, 38°00'E).  
493 Geladas live in multi-level societies, where several reproductive units (comprising a leader male,  
494 several adult females, their offspring, and occasionally 1–2 follower males) aggregate together  
495 during the day to forage and sleep together forming a “band”, sharing a homerange [80]. Since Jan  
496 2006, the Simien Mountains Gelada Research Project (SMGRP) has collected behavioral,  
497 demographic, and genetic data on a near-daily basis from over 600 individuals living in 2 separate  
498 bands of the area. All gelada subjects were habituated to human observers on foot and were  
499 individually recognizable. Data were derived from 89 infants and juveniles aged between 0-3 years  
500 old and 83 adult females living in 23 different reproductive units. The date of birth of each infant  
501 was known within a few days’ accuracy. The reproductive state of each adult female was  
502 monitored daily and recorded as cycling (as indicated by the presence of sex skin swellings on the  
503 neck, chest, and perineum), lactating (if she had a nursing infant), or pregnant (the date of  
504 conception was inferred by removing 183 days from the date of birth of subsequent offspring)  
505 [81]. Records of female reproductive history were used to assign maternal parity status for each

506 infant (first-time mother: primiparous or multi-time mother: multiparous) and to establish the date  
507 at which the mother resumed cycling following the infant's birth, which we used to estimate the  
508 approximate age at weaning for each infant. For 8 infants, age at weaning began on the date of  
509 maternal death.

510

511 ***Fecal sample collection***

512 Fecal samples (N=525; 303 females, 222 male samples) from 89 immature geladas (i.e., infants  
513 and juveniles sampled pre-reproductive maturity; female: N=51; male: N=38,  
514 mean $\pm$ SD=5.90 $\pm$ 5.53 samples per individual, range=1-18) were collected opportunistically from  
515 2015-2016, and then regularly from 2017 to 2018) during the development using targeted protocols  
516 (**Figure S1**). These samples come from individuals residing in 17 different reproductive units  
517 (mean $\pm$ SD= 5.65 $\pm$ 4.44 number of individuals sampled per unit, range=1-17). For a subset of  
518 immature samples (N=398 samples from 61 infants), we also collected a matched fecal sample  
519 from the mother (N=398 samples from 44 mothers) on the same day or on the following day of the  
520 infant sample collection. Fecal samples of known adult females in all reproductive states were also  
521 routinely collected (N=222 samples from 79 females) and were used to generate a random  
522 distribution of gut microbiome composition similarity between females of the population and  
523 immatures. Immediately upon defecation, approximately 1.5 g of feces was collected in 3 ml of  
524 RNA later [126] stored at room temperature for up to 2 months, and subsequently shipped to the  
525 University of Washington (UW). At UW, samples were stored at -80°C until the sequencing  
526 libraries were prepared.

527

528 ***Maternal dominance ranks***

529 Female dominance ranks were established using *ad libitum* and focal observations of agonistic  
530 interactions between all adult females belonging to the same unit with an Elo-rating procedure  
531 [127] implemented in the R package EloRating [128]. Agonistic interactions included physical  
532 aggression (hit, bite), chase, threats (vocal threats, non-vocal gestures), approach-avoid  
533 interactions (displacements) and submissive behaviors (fear bark, crouch, grimace). In geladas,  
534 agonistic interactions usually consist of a sequence of several behaviors in a row emitted and  
535 received by both parties. Since it can be difficult to establish the winner of each agonistic sequence,  
536 we consider each behavior of a sequence as a separate event and assign the winner and loser based  
537 on the directionality of the behavior. We obtained a daily Elo-score that we then averaged per  
538 month. Since Elo-scores can be sensitive to differences in sampling effort, we then converted this  
539 monthly Elo-rank into a monthly proportional rank and controlling for female group size  
540 (0=lowest-ranking females and 1= highest ranking female). In the analyses, we used maternal  
541 dominance rank during the month of the infant's birth since we expect microbially-mediated  
542 maternal effects to be the strongest in the postnatal period (during nursing). However, we also  
543 investigated maternal rank during pregnancy and at the date of immature sample collection, which  
544 led to similar results (not reported here).

545

#### 546 **Environmental data**

547 The study area is located at 3200 m above sea level and is characterized as an Afroalpine grassland  
548 ecosystem, consisting of grassland plateaus, scrublands, and Ericaceous forests [129]. The climate  
549 in the Simien Mountains National Park exhibits marked inter- and intra-annual fluctuation in  
550 rainfall and temperature and can be broadly divided into 3 distinct seasons : a cold-dry season (Oct  
551 to Jan), a hot-dry season (Feb to May) and a cold-wet season (Jun to Sep) [130]. Fecal samples of

552 immatures and adult females were collected across the year, with roughly equal coverage across  
553 seasons (406 in cold-dry, 426 in cold-wet and 313 in hot-dry season). Daily cumulative rainfall  
554 and minimum and maximum temperature are recorded on a near-daily basis by the SMGRP.  
555 Geladas are graminivorous, with up to 90% of their diet composed of graminoids [76]. They eat  
556 primarily graminoid leaves (i.e., grasses and sedges) all year long, but increase substantially their  
557 consumption of underground storage organs (rhizome, corms, roots) in the dry season, as above-  
558 ground graminoid leaves become less abundant [76]. A previous study established that the gut  
559 microbiome composition of adults shifts in response to environmental variation, in particular with  
560 cumulative rainfall which is a good proxy of diet. [79]. Thus, in all models we controlled the total  
561 cumulative rainfall over the 30 days prior to the date of fecal sample collection (as a proxy for  
562 grass availability) and the average minimum daily temperatures in the 30 days preceding the date  
563 of sample collection (as a proxy of thermoregulatory constraints).

564

#### 565 ***16S rRNA gene sequencing***

566 We performed 16S rRNA gene amplicon sequencing on the immature and female fecal samples to  
567 establish gut microbial composition. We first extracted microbial DNA using Qiagen's  
568 PowerLyzer PowerSoil DNA Isolation kit (Qiagen #12855) following standard protocols. We then  
569 amplified the hypervariable V4 region of the 16S rRNA gene using PCR primer set 515F and 806R  
570 from The Human Microbiome Project and a dual-indexing approach [131]. Details of the  
571 amplification protocol can be found in [79] (see also: <https://smack-lab.com/protocols/>). The  
572 libraries were then pooled in roughly equimolar amounts (each with their own unique indexing  
573 primer combination), spiked with 10% PhiX to increase library complexity, and sequenced

574 together on a single Illumina NovaSeq 6000 SP 250 bp paired-end sequence flowcell at the  
575 Northwest Genomics Sequencing Core at the University of Washington, Seattle.

576 Data were processed using the Quantitative Insights Into Microbial Ecology 2 (QIIME2)  
577 platform [132] using the demux command to demultiplex raw reads and the DADA2 pipeline [133]  
578 to generate amplicon sequence variants (ASVs) feature tables. Forward and reverse reads were  
579 trimmed to 220 and 180 bases, respectively, to remove the low-quality portion of the sequences.  
580 Only samples with more than 20,000 reads were retained for analyses following observation of  
581 rarefaction curves. After filtering, trimming, merging, and chimera removal, we retained a total of  
582 219,125,888 reads across the 525 immature fecal samples (417,382±645,328 reads per sample,  
583 range= 21,256- 7,976,983) and 293,003,271 reads across the 620 adult female fecal samples  
584 (472,586±869,181 reads per sample, range= 20,068- 10,723,460). ASVs were taxonomically  
585 assigned using the q2-feature classifier in QIIME2 against version 132 of the SILVA database  
586 (updated December 2017) [134] based on 100% similarity.

587

### 588 ***Statistical analyses***

589 The count and taxonomy files generated by QIIME2 were imported into R version 3.5.2 [135]  
590 using the qiime2R package [136]. We filtered the count table to retain only ASVs that had at least  
591 500 reads total in the dataset to eliminate potentially artifactual sequences. With this filtering  
592 criteria, only 3,884 ASVs remained (out of the 29,686 initially observed). In total, 3,784 different  
593 ASVs were found across the 525 immature fecal samples (mean±SD number of ASVs per sample:  
594 728±261, range: 65-1498), while the 620 female samples contained 3,679 ASVs (mean±SD  
595 number of ASVs per sample: 829±248, range: 98-1761). Most ASVs could be taxonomically

596 assigned to the phylum (100%), class (99%), and order levels (99%), with assignments decreasing  
597 substantially at the family (88%) and genus (63%) levels.

598

599 Alpha-diversity analyses

600 We calculated three complementary metrics of alpha diversity for each sample: the observed  
601 richness (the total number of unique ASVs per sample), Shannon Index (taking into account both  
602 richness and evenness in abundance of ASVs), and Faith's phylogenetic diversity (a measure of  
603 the diversity of phylogenetic lineages within a sample) using the "phyloseq" [137] and "picante"  
604 package [138]. To assess which predictors affected immatures' gut microbial alpha diversity, we  
605 used generalized additive mixed models (GAMMs) with the 'mgcv' package in R [139]. Such  
606 models allow fitting of a nonlinear relationship between the response variable and the fixed effect  
607 (by adding a smooth term), such as between alpha diversity and immature age (**Figure 1C**). Fitted  
608 predictors included: immature age at the date of fecal sample collection (modeled as a smooth  
609 term), immature sex, the parity status of mother, maternal dominance rank in the month of infant's  
610 birth, cumulative monthly rainfall, average monthly minimum temperature and the log-  
611 transformed sequencing depth (i.e., the number of reads per sample). The use of rarefaction (i.e.,  
612 subsampling of the read counts in each sample to a common sequencing depth) has been strongly  
613 discouraged on microbiome dataset because it discards too much sequencing information and leads  
614 to high rate of false positives [140], so we calculated alpha diversity on raw counts but controlled  
615 for sequencing depth in our model. Graphical representation of alpha diversity metrics are  
616 nonetheless displayed using a rarefied dataset at 20,000 reads. Individual identity and unit  
617 membership were included as random effects. Model residual checks were performed using the  
618 qq.gamViz and check.gamViz functions. Given that GAMMs models can not accommodate the

619 test of the interaction between a smooth and fixed term, we ran those models including all  
620 immature samples or on only young infants (0-12 months) to test for the significance of maternal  
621 effects in early life (i.e., when the infant is still nursing).

622 To quantitatively assess the age at which alpha diversity reaches a plateau (i.e., converges  
623 to adult-like pattern), we used quadratic plateau models (formula:  $y \sim (a + b * x + c * I(x^2)) * (x$   
624  $\leq -0.5 * b/c) + (a + I(-b^2/(4 * c))) * (x > -0.5 * b/c))$  fitted using the `nlsfit()` function of the  
625 `easynls` package [141] and extracted the critical point of inflection and r-squared of the optimized  
626 model (i.e., with the values of a, b and c fit best the data). Since it is not possible to control for  
627 covariates in those analyses (e.g., sequencing depth), we ran those models on a rarefied dataset at  
628 20,000 reads.

629

### 630 Beta-diversity analyses

631 Beta-diversity (between-sample dissimilarity in composition) was computed as the Aitchison  
632 distance [142], which is simply the Euclidean distance between samples after centered log-ratio  
633 (clr) transformation of the raw counts (a pseudo-count was added to the zeros using the imputation  
634 based on a Bayesian-multiplicative replacement from the `cmultRepl()` function in the package  
635 `zCompositions` [143]). The clr transformation allows us to account for differences in sequencing  
636 depth between samples and is a better practice than rarefaction of the counts [144]. Principal  
637 components analysis (PCA) on the Aitchison dissimilarity matrix (function “`prcomp`”) was used  
638 to examine how immatures samples clustered by age. We extracted the loading scores for each  
639 ASV onto the first Principal component (PC1) of the PCA to determine which specific ASVs have  
640 the highest influence on the clustering by age of samples. A quadratic plateau model was  
641 implemented to find the age at which Aitchison beta diversity reaches a plateau.

642 Permutational Multivariate Analysis of Variance (PERMANOVA) was then carried out on  
643 the Aitchison dissimilarity matrix using the adonis2 function in the vegan package [145] (with  
644 10,000 permutations) to test for associations among gut microbial beta-diversity and the variables  
645 of interest (immature age, sex, maternal parity, maternal rank, environmental variables, the log-  
646 transformed sequencing depth, and unit membership). Individual identity was included as a  
647 blocking factor (“strata”) to control for repeated sampling among individuals. PERMANOVA  
648 models were run when including all immatures samples or on only young infants (0-12 months) to  
649 test for the significance of maternal effects in early life. We also replicated those PERMANOVA  
650 analyses using more classical measures of beta diversity (unweighted and weighted UniFrac  
651 dissimilarity) on a rarefied dataset at 20,000 reads and found essentially similar results (**Table**  
652 **S13**).

653

654 Mother-infant comparison of gut microbiome composition

655 To assess similarity in gut microbiome composition between mother and offspring, we calculated  
656 (1) the number of shared ASVs across maternal and immature communities, and (2) the beta  
657 diversity dissimilarity (unweighted and weighted UniFrac distances) between the matched infant-  
658 mother fecal samples collected the same day (N=398). The dataset of immature and mother fecal  
659 samples was rarefied at 20,000 reads to calculate these metrics since sequencing depth is likely to  
660 affect the similarity between paired samples. Quadratic plateau models were implemented on the  
661 three metrics to identify the age at which infants converged toward the maternal (i.e., adult-like)  
662 gut microbial composition. To assess which predictors affected the compositional similarity  
663 between mother-offspring pairs, we used GAMMs to model those three metrics as a function of  
664 immature age (as a smooth term), immature sex, maternal parity and maternal dominance rank,

665 climatic variables (cumulative monthly rainfall and average monthly minimum temperature),  
666 while individual identity and unit membership were included as random effects. These GAMMs  
667 were also run separately on young infant samples (<12 months) or only on old immatures (>18  
668 months) to assess how the strength of vertical transmission varies with maternal traits.

669

670 Individuality of the microbiomes in immatures

671 To capture the compositional divergence between immature samples, we calculated a measure of  
672 “individuality” of the microbiomes among the 525 immature samples, as defined in [146], which  
673 corresponds to the beta diversity dissimilarity value between a sample and the most similar sample  
674 (i.e., the minimum pairwise values from a beta diversity dissimilarity matrix, based on unweighted  
675 and weighted UniFrac metrics). The higher the value, the more distinct the gut microbiome  
676 composition is from all other immature samples in the cohort. This was calculated using the  
677 rarefied dataset at 20,000 reads.

678

679 Age-associated changes in microbial taxonomic composition

680 To identify the microbial taxa that vary significantly in abundance as immatures age, we used a  
681 statistical framework that is commonly used to analyze time series (and, in our case, longitudinal  
682 dataset). Autoregressive Integrated Moving Average (ARIMA) models allowed us to model and  
683 test for chronological trends in temporal data [147]. First, raw microbial counts were aggregated  
684 at the family or genus level, normalized using a clr-transformation, and z-transformed per taxon  
685 (i.e., across samples) to correct for variation in library size and unaccounted variance due to other  
686 covariates. Only microbial families or genera  $\geq 0.01\%$  relative abundance across the samples were  
687 selected for further analyses. Second, the counts were averaged across samples belonging to the

688 same chronological age and converted into z-ordered objects (using R package zoo [148]) and into  
689 time series objects. Formatted time series were then analyzed using auto.arima (from the forecast  
690 R package [149]), using stepwise search and Akaike Information Criterion (AIC) to select the best  
691 model. This algorithm scans a wide range of possible ARIMA models and selects the one with the  
692 smallest AIC. ARIMA models that exhibited significant non-stationary trends (as opposed to  
693 unstructured “noise” fluctuations indistinguishable from stationary data) were selected following  
694 the criteria in [147]: (1) the difference order from stationary was higher than zero, and (2) at least  
695 one autoregressive (AR) and moving average (MA) coefficient was included in the model. LOESS  
696 regressions were then fitted to re-predict the count of each taxon as a function of age.

697 We then grouped bacterial taxa into clusters based on similarities in age-associated  
698 abundance trajectories. Pairwise distances between microbial taxa trajectories (i.e., the predicted  
699 values of the LOESS regression) were computed using correlation coefficients as a distance  
700 measure [150], and hierarchical clustering was performed using the complete method (using the  
701 function hclust from the stats R package). The optimal number of clusters was determined using  
702 the Elbow method (i.e., choosing a number of clusters so that adding another cluster does not  
703 highly improve the total within-cluster sum of squares) [151]. Results of hierarchical clustering  
704 were visualized using the R package heatmap3 [152] to provide an overview of gut microbiome  
705 composition changes with age.

706

#### 707 Age-associated changes in microbial functional composition

708 To predict the microbial functional metagenomes of each sample from 16S rRNA data, we used  
709 Phylogenetic Investigation of Communities by Reconstruction of Unobserved States 2  
710 (PICRUSt2) v.2.1.3-b software [84] with default options (picrust2\_pipeline.py). We then

711 computed the relative abundance of Kyoto Encyclopedia of Genes and Genomes (KEGG)  
712 Orthologs (KOs) (agglomerated at level 2 or 3 of the BRITE map) and of Enzyme Commission  
713 (EC) numbers for each sample. The accuracy of the PICRUSt2 predictions for each sample were  
714 assessed by calculating the weighted Nearest Sequence Taxon Index (NSTI) score, a measure of  
715 how similar the bacteria from the sample are to reference genome sequences. The mean $\pm$ SD NSTI  
716 score across the 525 immature samples was  $0.49 \pm 0.19$  (range: 0.01-0.89).

717 The age-related temporal trajectory of each KO pathway and EC was assessed using  
718 ARIMA models in a similar fashion than described above. The only difference is that the raw  
719 metagenome counts were transformed into relative abundance (instead of clr transformed). Only  
720 microbial pathways  $\geq 0.01\%$  relative abundance across the samples were included. Hierarchical  
721 clustering was used to group the pathways with similar aging trajectories.

722

### 723 Maternal effects on offspring's gut microbiome development

724 We examined how maternal traits (dominance rank, parity) were associated with differences in  
725 offspring gut microbiome (1) composition (at the family and genus levels) and (2) function (KO  
726 pathways at level 2 or 3 and EC numbers) using GAMMs models. We modelled the relative  
727 abundance of each taxon and each functional pathway as a function of maternal parity and maternal  
728 dominance rank in the month of infant's birth, while controlling for immature age (as a smooth  
729 term), immature sex, climatic variables (cumulative monthly rainfall and average monthly  
730 minimum temperature. For (1), the logarithm of the relative abundance of each taxon was fit  
731 (adding a pseudo-count of 0.001% to include zero counts). In all models, individual identity and  
732 unit membership were included as random effects. P-values were adjusted for multiple hypothesis  
733 testing by calculating the Benjamini-Hochberg FDR multiple-test correction. Only taxa that had

734 an average relative abundance across samples  $\geq 0.01\%$  were tested. Given the number of metabolic  
735 pathways and the correction of p-values for multiple testings, only pathways that had an average  
736 relative abundance across samples  $\geq 0.10\%$  were tested. Taxa or functional pathways with a p-  
737 value  $< 0.05$  were considered statistically significant. These analyses were run including all  
738 immatures samples (0-3 years), only young infant samples (<12months) or only old samples (>18  
739 months).

740

741 Mother-to-infant vertical transmission

742 To assess if maternal and infant gut microbiome communities were more similar than expected by  
743 chance, we took a resampling approach (with 1000 repetitions) to compare the number of shared  
744 ASVs and beta diversity dissimilarity metrics (unweighted and weighted UniFrac) between (1)  
745 actual mother-infant matched samples (the observed value) and (2) random pairs of fecal samples  
746 of an infant and an adult female of the population (the random distribution). Since mother-infant  
747 pairs always shared the same social unit and were always collected 0-1 day apart (i.e., in the same  
748 season), we needed to match the random female samples accordingly to avoid introducing  
749 consistent bias in the random distribution. The random matching was thus done by either matching  
750 the infant sample to (i) a female of the same unit (to control for higher similarity only due to  
751 sharing the same social group) or (ii) a female sample collected in the same season (to control for  
752 higher similarity only due to seasonality). We did not have enough female samples to match by  
753 both criteria simultaneously. After we created the set of random pairs, we use GAMMs to compare  
754 the observed and random distribution of the metrics (number of shared ASVs or beta diversity  
755 dissimilarity) (response variable) by fitting a variable (“type of pairs?”) coding whether the value  
756 comes from an actual mother-offspring pair (1=observed) or a random infant-female pair

757 (0=random), and controlling for immature age (as a smooth term) and immature sex. Infant and  
758 female identity were included as random effects to account for repeated observations of the same  
759 individuals. We extracted the estimate of the “type of pairs?” variable for the model and re-ran the  
760 model on a different set of random pairs (1000 times in total). We thus obtained a distribution of  
761 1000 estimates for the “type of pairs?” variable. We report the exact p-value (calculated as the  
762 proportion of models with positive estimates for the number of shared ASVs and the proportion of  
763 models with negative estimates for beta dissimilarity) and the 95% confidence interval of the  
764 estimates of the “type of pairs?” variable. Fecal samples were rarefied at 20,000 reads to control  
765 for differences in sequence depth between infant and female samples. These analyses were run  
766 including all immatures samples (0-3 years), only young infant samples (0-12 months), or only old  
767 immatures (>18 months) to compare the strength of the effect among the different age categories.

768 To examine the nature of the shared microbes between mother and offspring in early life  
769 (when infants are <12 months), we extracted all ASVs in common between the 136 mother-  
770 offspring pairs (on the rarefied dataset). For each ASV found in the young infant samples (<12  
771 months, N=3,402 ASVs total), we simply computed its relative abundance and prevalence across  
772 samples and how many pairs shared this given ASV. We then plotted the loading score of the ASV  
773 on PC1 of the beta diversity ordination (PC1 correlates strongly with age, so ASVs with the most  
774 negative versus positive loading scores are found in early versus later life) according to the  
775 percentage of mother-offspring pairs sharing this ASV.

776

## 777 **ACKNOWLEDGEMENTS**

778 We thank the Ethiopian Wildlife Conservation Authority (EWCA), along with the wardens and  
779 staff of the Simien Mountains National Park for permission to conduct research and ongoing

780 support to our long-term research project. We are also very grateful to the Simien Mountains  
781 Gelada Research Project field team for their help with field data collection, particularly our  
782 primary data collectors (Esheti Jejaw, Ambaye Fanta, Setey Girmay, Atirsaw Adugna, Dereje  
783 Bewket) and research assistants in the field (in particular Liz Babbitt, Maddie Melton). We would  
784 like to thank Marina Watowich and Dr. Kenneth Chiou for helpful discussions on ARIMA  
785 analyses.

786

## 787 **AUTHORS' CONTRIBUTIONS**

788 Conceptualization, Data curation, Formal analysis, Investigation, Visualization: A.B, A.L., N.S.M;  
789 Methodology/Laboratory work: A.B., S.S., A.M., Writing – Original Draft: A.B, A.L., N.S.M;  
790 Writing – Review & Editing: all authors; Funding Acquisition: A.L., N.S.M., J.C.B., T.J.B., L.R.;  
791 Supervision: A.L. and N.S.M.

792

## 793 **FUNDING**

794 This research was funded by the National Science Foundation (BCS-1723228, BCS-1723237).  
795 The long-term gelada research was supported by the National Science Foundation (BCS-2010309,  
796 BCS-0715179, IOS-1255974, IOS-1854359), the National Geographic Society (8100-06, 8989-  
797 11, NGS-50409R-18), the Leakey Foundation (A.L., J.B., T.B.), the University of Michigan, Stony  
798 Brook University, and Arizona State University.

799

## 800 **AVAILABILITY OF DATA AND MATERIALS**

801 All 16S sequence data used in this study are available at the NCBI Sequence Read Archive under  
802 BioProject ID: PRJNA772269 (<http://www.ncbi.nlm.nih.gov/bioproject/772269>) for the immature

803 samples [temporary note: the sequences coming from these samples have been deposited on  
804 NCBI, but will only be released upon acceptance of the manuscript] and PRJNA639843  
805 (<https://www.ncbi.nlm.nih.gov/bioproject/PRJNA639843>) for the adult female samples. Data  
806 (including the ASV table and metadata) and R code to reproduce all the analyses are available at:  
807 [https://github.com/GeladaResearchProject/Baniel-et-al\\_2022\\_Infant-gut-microbiome](https://github.com/GeladaResearchProject/Baniel-et-al_2022_Infant-gut-microbiome).

808

## 809 COMPETING INTERESTS

810 The authors declare no competing interests.

811

## 812 REFERENCES

- 813 1. Kurokawa K, Itoh T, Kuwahara T, Oshima K, Toh H, Toyoda A, et al. Comparative  
814 metagenomics revealed commonly enriched gene sets in human gut microbiomes. *DNA*  
815 *Research*. 2007;14: 169–181.
- 816 2. Koenig JE, Spor A, Scalfone N, Fricker AD, Stombaugh J, Knight R, et al. Succession of  
817 microbial consortia in the developing infant gut microbiome. *PNAS*. 2011;108: 4578–4585.
- 818 3. Palmer C, Bik EM, DiGiulio DB, Relman DA, Brown PO. Development of the human  
819 infant intestinal microbiota. *PLoS Biol*. 2007;5: e177.
- 820 4. Guittar J, Shade A, Litchman E. Trait-based community assembly and succession of the  
821 infant gut microbiome. *Nat Commun*. 2019;10: 1–11.
- 822 5. Bäckhed F, Roswall J, Peng Y, Feng Q, Jia H, Kovatcheva-Datchary P, et al. Dynamics and  
823 stabilization of the human gut microbiome during the first year of life. *Cell Host Microbe*.  
824 2015;17: 690–703.
- 825 6. Roswall J, Olsson LM, Kovatcheva-Datchary P, Nilsson S, Tremaroli V, Simon M-C, et al.  
826 Developmental trajectory of the healthy human gut microbiota during the first 5 years of  
827 life. *Cell Host Microbe*. 2021;29: 765–776.e3.
- 828 7. Sharon I, Morowitz MJ, Thomas BC, Costello EK, Relman DA, Banfield JF. Time series  
829 community genomics analysis reveals rapid shifts in bacterial species, strains, and phage  
830 during infant gut colonization. *Genome Res*. 2013. pp. 111–120.
- 831 8. de Muinck EJ, Trosvik P. Individuality and convergence of the infant gut microbiota during  
832 the first year of life. *Nat Commun*. 2018;9: 1–8.

833 9. Mach N, Berri M, Estellé J, Levenez F, Lemonnier G, Denis C, et al. Early-life  
834 establishment of the swine gut microbiome and impact on host phenotypes. *Environmental*  
835 *microbiology reports*. 2015;7: 554–569.

836 10. Petrullo L, Baniel A, Jorgensen MJ, Sams S, Snyder-Mackler N, Lu A. Early life gut  
837 microbiome dynamics mediate maternal effects on infant growth in rhesus monkeys.  
838 <https://www.biorxiv.org/content/10.1101/2021.05.11.443657v1>

839 11. Videvall E, Song SJ, Bensch HM, Strandh M, Engelbrecht A, Serfontein N, et al. Major  
840 shifts in gut microbiota during development and its relationship to growth in ostriches.  
841 *Molecular Ecology*. 2019;28: 2653–2667.

842 12. Sommer F, Bäckhed F. The gut microbiota – masters of host development and physiology.  
843 *Nat Rev Microbiol*. 2013;11: 227–238.

844 13. Heiss CN, Olofsson LE. The role of the gut microbiota in development, function and  
845 disorders of the central nervous system and the enteric nervous system. *Journal of*  
846 *neuroendocrinology*. 2019;31: e12684.

847 14. Clarke G, O’Mahony SM, Dinan TG, Cryan JF. Priming for health: gut microbiota acquired  
848 in early life regulates physiology, brain and behaviour. *Acta Paediatrica*. 2014;103: 812–  
849 819.

850 15. Gensollen T, Iyer SS, Kasper DL, Blumberg RS. How colonization by microbiota in early  
851 life shapes the immune system. *Science*. 2016;352: 539–544.

852 16. Gollwitzer ES, Marsland BJ. Impact of early-life exposures on immune maturation and  
853 susceptibility to disease. *Trends Immunol*. 2015;36: 684–696.

854 17. Warne RW, Kirschman L, Zeglin L. Manipulation of gut microbiota during critical  
855 developmental windows affects host physiological performance and disease susceptibility  
856 across ontogeny. *Journal of Animal Ecology*. 2019;88: 845–856.

857 18. Arrieta M-C, Stiemsma LT, Amenyogbe N, Brown EM, Finlay B. The intestinal  
858 microbiome in early life: health and disease. *Front Immunol*. 2014;5: 427.

859 19. Stiemsma LT, Michels KB. The role of the microbiome in the developmental origins of  
860 health and disease. *Pediatrics*. 2018;141.

861 20. Risnes KR, Belanger K, Murk W, Bracken MB. Antibiotic exposure by 6 months and  
862 asthma and allergy at 6 years: findings in a cohort of 1,401 US children. *American journal*  
863 *of epidemiology*. 2011;173: 310–318.

864 21. Yallapragada SG, Nash CB, Robinson DT. Early-life exposure to antibiotics, alterations in  
865 the intestinal microbiome, and risk of metabolic disease in children and adults. *Pediatric*  
866 *Annals*. 2015.

867 22. Rautava S. Early-life antibiotic exposure, the gut microbiome, and disease in later life. The

868 Human microbiome in early Life. Academic Press. 2021. pp. 135–153.

869 23. Ungaro R, Bernstein CN, Gearry R, Hviid A, Kolho K-L, Kronman MP, et al. Antibiotics  
870 associated with increased risk of new-onset Crohn's disease but not ulcerative colitis: a  
871 meta-analysis. American Journal of Gastroenterology. 2014. pp. 1728–1738.

872 24. Bauer H, Horowitz RE, Levenson SM, Popper H. The response of the lymphatic tissue to  
873 the microbial flora. Studies on germfree mice. Am J Pathol. 1963;42: 471–483.

874 25. Olszak T, An D, Zeissig S, Vera MP, Richter J, Franke A, et al. Microbial exposure during  
875 early life has persistent effects on natural killer T cell function. Science. 2012;336: 489–  
876 493.

877 26. Cox LM, Yamanishi S, Sohn J, Alekseyenko AV, Leung JM, Cho I, et al. Altering the  
878 intestinal microbiota during a critical developmental window has lasting metabolic  
879 consequences. Cell. 2014;158: 705–721.

880 27. Aidy SE, El Aidy S, Hooiveld G, Tremaroli V, Bäckhed F, Kleerebezem M. The gut  
881 microbiota and mucosal homeostasis. Gut Microbes. 2013. pp. 118–124.

882 28. Kozakova H, Schwarzer M, Tuckova L, Srutkova D, Czarnowska E, Rosiak I, et al.  
883 Colonization of germ-free mice with a mixture of three *Lactobacillus* strains enhances the  
884 integrity of gut mucosa and ameliorates allergic sensitization. Cell Mol Immunol. 2016;13:  
885 251–262.

886 29. Moore RE, Townsend SD. Temporal development of the infant gut microbiome. Open Biol.  
887 2019;9: 190128.

888 30. Vandenplas Y, Carnielli VP, Ksiazek J, Luna MS, Migacheva N, Mosselmans JM, et al.  
889 Factors affecting early-life intestinal microbiota development. Nutrition. 2020;78: 110812.

890 31. Dwivedi M, Ansarullah, Radichev I, Kemp EH. Alteration of immune-mechanisms by  
891 human microbiota and development and prevention of human diseases. J Immunol Res.  
892 2017;2017: Article ID 6985256.

893 32. Schloss PD, Schubert AM, Zackular JP, Iverson KD, Young VB, Petrosino JF. Stabilization  
894 of the murine gut microbiome following weaning. Gut Microbes. 2012;3: 383–393.

895 33. Charbonneau MR, O'Donnell D, Blanton LV, Totten SM, Davis JCC, Barratt MJ, et al.  
896 Sialylated milk oligosaccharides promote microbiota-dependent growth in models of infant  
897 undernutrition. Cell. 2016;164: 859–871.

898 34. Foong JPP, Hung LY, Poon S, Savidge TC, Bernstein JC. Early life interaction between the  
899 microbiota and the enteric nervous system. Am J Physiol Gastrointest Liver Physiol.  
900 2020;319: G541–G548.

901 35. Kennedy EA, King KY, Baldridge MT. Mouse microbiota models: comparing germ-free  
902 mice and antibiotics treatment as tools for modifying gut bacteria. Front Physiol. 2018;9:

903 1534.

904 36. Beaumont M, Paës C, Mussard E, Knudsen C, Cauquil L, Aymard P, et al. Gut microbiota  
905 derived metabolites contribute to intestinal barrier maturation at the suckling-to-weaning  
906 transition. *Gut Microbes*. 2020;3: 1–9.

907 37. Frese SA, Parker K, Calvert CC, Mills DA. Diet shapes the gut microbiome of pigs during  
908 nursing and weaning. *Microbiome*. 2015;3: 28.

909 38. Meale SJ, Li S, Azevedo P, Derakhshani H, Plaizier JC, Khafipour E, et al. Development of  
910 ruminal and fecal microbiomes are affected by weaning but not weaning strategy in dairy  
911 calves. *Front Microbiol*. 2016;7: 582.

912 39. Berry ASF, Pierdon MK, Misic AM, Sullivan MC, O'Brien K, Chen Y, et al. Remodeling  
913 of the maternal gut microbiome during pregnancy is shaped by parity. *Microbiome*. 2021;9:  
914 1–5.

915 40. Pascoe EL, Hauffe HC, Marchesi JR, Perkins SE. Network analysis of gut microbiota  
916 literature: an overview of the research landscape in non-human animal studies. *ISME J*.  
917 2017;11: 2644–2651.

918 41. Amato KR. Co-evolution in context: The importance of studying gut microbiomes in wild  
919 animals. *Microbiome Sci Med*. 2013;1.

920 42. Wang S, Ryan CA, Boyaval P, Dempsey EM, Ross RP, Stanton C. Maternal vertical  
921 transmission affecting early-life microbiota development. *Trends Microbiol*. 2020;28: 28–  
922 45.

923 43. McDonald B, McCoy KD. Maternal microbiota in pregnancy and early life. *Science*.  
924 2019;365: 984–985.

925 44. Ferretti P, Pasolli E, Tett A, Asnicar F, Gorfer V, Fedi S, et al. Mother-to-infant microbial  
926 transmission from different body sites shapes the developing infant gut microbiome. *Cell Host Microbe*.  
927 2018;24: 133–145.e5.

928 45. Mueller NT, Bakacs E, Combellick J, Grigoryan Z, Dominguez-Bello MG. The infant  
929 microbiome development: Mom matters. *Trends Mol Med*. 2015;21: 109–117.

930 46. Funkhouser LJ, Bordenstein SR. Mom knows best: the universality of maternal microbial  
931 transmission. *PLoS Biol*. 2013;11: e1001631.

932 47. Mallott EK, Amato KR. Host specificity of the gut microbiome. *Nat Rev Microbiol*.  
933 2021;19: 639–653.

934 48. Bokulich NA, Chung J, Battaglia T, Henderson N, Jay M, Li H, et al. Antibiotics, birth  
935 mode, and diet shape microbiome maturation during early life. *Science Translational  
936 Medicine*. 2016. pp. 343ra82–343ra82.

937 49. Jost T, Lacroix C, Braegger CP, Rochat F, Chassard C. Vertical mother-neonate transfer of  
938 maternal gut bacteria via breastfeeding. *Environ Microbiol.* 2014;16: 2891–2904.

939 50. Pannaraj PS, Li F, Cerini C, Bender JM, Yang S, Rollie A, et al. Association between breast  
940 milk bacterial communities and establishment and development of the infant gut  
941 microbiome. *JAMA Pediatr.* 2017;171: 647–654.

942 51. Zivkovic AM, German JB, Lebrilla CB, Mills DA. Human milk glycobiome and its impact  
943 on the infant gastrointestinal microbiota. *PNAS.* 2011;108: 4653–4658.

944 52. Pacheco AR, Barile D, Underwood MA, Mills DA. The impact of the milk glycobiome on  
945 the neonate gut microbiota. *Annu Rev Anim Biosci.* 2015;3: 419–445.

946 53. Newburg DS, Morelli L. Human milk and infant intestinal mucosal glycans guide  
947 succession of the neonatal intestinal microbiota. *Pediatr Res.* 2015;77: 115–120.

948 54. Murphy K, Curley D, O'Callaghan TF, O'Shea C-A, Dempsey EM, O'Toole PW, et al. The  
949 composition of human milk and infant faecal microbiota over the first three months of life:  
950 a pilot study. *Sci Rep.* 2017;7: 40597.

951 55. Asnicar F, Manara S, Zolfo M, Truong DT, Scholz M, Armanini F, et al. Studying vertical  
952 microbiome transmission from mothers to infants by strain-level metagenomic profiling.  
953 *mSystems.* 2017;2.

954 56. Korpela K, Costea P, Coelho LP, Kandels-Lewis S, Willemse G, Boomsma DI, et al.  
955 Selective maternal seeding and environment shape the human gut microbiome. *Genome  
956 Res.* 2018;28: 561–568.

957 57. Perez PF, Doré J, Leclerc M, Levenez F, Benyacoub J, Serrant P, et al. Bacterial imprinting  
958 of the neonatal immune system: lessons from maternal cells? *Pediatrics.* 2007;119: e724–  
959 32.

960 58. Sarkar A, Harty S, Johnson KV, Moeller AH, Archie EA, Schell LD, et al. Microbial  
961 transmission in animal social networks and the social microbiome. *Nature Ecology  
962 Evolution.* 2020;22: 1–6.

963 59. Sprockett D, Fukami T, Relman DA. Role of priority effects in the early-life assembly of  
964 the gut microbiota. *Nat Rev Gastroenterol Hepatol.* 2018;15: 197–205.

965 60. Bogado Pascottini O, Spricigo JFW, Van Schyndel SJ, Mion B, Rousseau J, Weese JS, et al.  
966 Effects of parity, blood progesterone, and non-steroidal anti-inflammatory treatment on the  
967 dynamics of the uterine microbiota of healthy postpartum dairy cows. *PLoS One.* 2021;16:  
968 e0233943.

969 61. Marcabal A, Barboza M, Sonnenburg ED, Pudlo N, Martens EC, Desai P, et al. *Bacteroides*  
970 in the infant gut consume milk oligosaccharides via mucus-utilization pathways. *Cell Host  
971 Microbe.* 2011;10: 507–514.

972 62. Marcobal A, Barboza M, Froehlich JW, Block DE, German JB, Lebrilla CB, et al.  
973 Consumption of human milk oligosaccharides by gut-related microbes. *J Agric Food Chem.*  
974 2010;58: 5334–5340.

975 63. Hinde K, Power ML, Oftedal OT. Rhesus macaque milk: magnitude, sources, and  
976 consequences of individual variation over lactation. *Am J Phys Anthropol.* 2009;138: 148–  
977 157.

978 64. Hinde K, Milligan LA. Primate milk: proximate mechanisms and ultimate perspectives.  
979 *Evol Anthropol.* 2011;20: 9–23.

980 65. Lu A, Petrullo L, Carrera S, Feder J, Schneider-Crease I, Snyder-Mackler N.  
981 Developmental responses to early-life adversity: evolutionary and mechanistic perspectives.  
982 *Evol Anthropol.* 2019;28: 249–266.

983 66. Stanton MA, Lonsdorf EV, Murray CM, Pusey AE. Consequences of maternal loss before  
984 and after weaning in male and female wild chimpanzees. *Behav Ecol Sociobiol.* 2020;74:  
985 22.

986 67. Tung J, Archie EA, Altmann J, Alberts SC. Cumulative early life adversity predicts  
987 longevity in wild baboons. *Nat Commun.* 2016;7: 1–7.

988 68. Zipple MN, Archie EA, Tung J, Altmann J, Alberts SC. Intergenerational effects of early  
989 adversity on survival in wild baboons. *eLife.* 2019;24: e47433.

990 69. Silk JB, Beehner JC, Bergman TJ, Crockford C, Engh AL, Moscovice LR, et al. The  
991 benefits of social capital: close social bonds among female baboons enhance offspring  
992 survival. *Proc. Royal Soc. B: Biological Sciences.* 2009;276: 3099–3104.

993 70. Maestripieri D. Maternal influences on primate social development. *Behav Ecol Sociobiol.*  
994 2018;72: 1–12.

995 71. Altmann J, Alberts SC. Growth rates in a wild primate population: ecological influences  
996 and maternal effects. *Behav Ecol Sociobiol.* 2005;57: 490–501.

997 72. Stoffel MA, Acevedo-Whitehouse K, Morales-Durán N, Grosser S, Chakarov N, Krüger O,  
998 et al. Early sexual dimorphism in the developing gut microbiome of northern elephant seals.  
999 *Mol Ecol.* 2020;29: 2109–2122.

1000 73. Janiak MC, Montague MJ, Villamil CI, Stock MK, Trujillo AE, DePasquale AN, et al. Age  
1001 and sex-associated variation in the multi-site microbiome of an entire social group of free-  
1002 ranging rhesus macaques. *Microbiome.* 2021;9: 1–17.

1003 74. Reese AT, Phillips SR, Owens LA, Venable EM, Langergraber KE, Machanda ZP, et al.  
1004 Age patterning in wild chimpanzee gut microbiota diversity reveals differences from  
1005 humans in early life. *Curr Biol.* 2021;31: 613–620.e3.

1006 75. McKenney EA, Rodrigo A, Yoder AD. Patterns of gut bacterial colonization in three

1007 primate species. PLoS One. 2015;10: e0124618.

1008 76. Jarvey JC, Low BS, Pappano DJ, Bergman TJ, Beehner JC. Graminivory and fallback  
1009 foods: annual diet profile of geladas (*Theropithecus gelada*) living in the Simien Mountains  
1010 National Park, Ethiopia. Int J Primatol. 2018;39: 105–126.

1011 77. Fashing PJ, Nguyen N, Venkataraman VV, Kerby JT. Gelada feeding ecology in an intact  
1012 ecosystem at Guassa, Ethiopia: Variability over time and implications for theropith and  
1013 hominin dietary evolution. Am J Phys Anthropol. 2014;155: 1–16.

1014 78. Trosvik P, de Muinck EJ, Rueness EK, Fashing PJ, Beierschmitt EC, Callingham KR, et al.  
1015 Multilevel social structure and diet shape the gut microbiota of the gelada monkey, the only  
1016 grazing primate. Microbiome. 2018;6: 84.

1017 79. Baniel A, Amato KR, Beehner JC, Bergman TJ, Mercer A, Perlman RF, et al. Seasonal  
1018 shifts in the gut microbiome indicate plastic responses to diet in wild geladas. Microbiome.  
1019 2021;9: 1–20.

1020 80. Snyder-Mackler N, Beehner JC, Bergman TJ. Defining higher levels in the multilevel  
1021 societies of geladas (*Theropithecus gelada*). Int J Primatol. 2012;33: 1054–1068.

1022 81. Roberts EK, Lu A, Bergman TJ, Beehner JC. Female reproductive parameters in wild  
1023 geladas (*Theropithecus gelada*). Int J Primatol. 2017;38: 1–20.

1024 82. Milani C, Duranti S, Bottacini F, Casey E, Turroni F, Mahony J, et al. The first microbial  
1025 colonizers of the human gut: composition, activities, and health implications of the infant  
1026 gut microbiota. Microbiol Mol Biol Rev. 2017;81: 1–67.

1027 83. Derrien M, Alvarez A-S, de Vos WM. The gut microbiota in the first decade of life. Trends  
1028 Microbiol. 2019;27: 997–1010.

1029 84. Douglas GM, Maffei VJ, Zaneveld JR, Yurgel SN, Brown JR, Taylor CM, et al. PICRUSt2  
1030 for prediction of metagenome functions. Nat Biotechnol. 2020;38: 685–688.

1031 85. Korpela K, de Vos WM. Early life colonization of the human gut: microbes matter  
1032 everywhere. Curr Opin Microbiol. 2018;44: 70–78.

1033 86. Cavalli C, Teng C, Battaglia FC, Bevilacqua G. Free sugar and sugar alcohol concentrations  
1034 in human breast milk. J Pediatr Gastroenterol Nutr. 2006;42: 215–221.

1035 87. Fox JG, Boutin SR, Handt LK, Taylor NS, Xu S, Rickman B, et al. Isolation and  
1036 characterization of a novel *Helicobacter* species, “*Helicobacter macacae*”, from rhesus  
1037 monkeys with and without chronic idiopathic colitis. Journal of Clinical Microbiology.  
1038 2007. pp. 4061–4063.

1039 88. Nielsen HL, Engberg J, Ejlertsen T, Nielsen H. Clinical manifestations of *Campylobacter*  
1040 *concisus* infection in children. Pediatr Infect Dis J. 2013;32: 1194–1198.

1041 89. Klein BS, Vergeront JM, Blaser MJ, Edmonds P, Brenner DJ, Janssen D, et al.  
1042 *Campylobacter* infection associated with raw milk. An outbreak of gastroenteritis due to  
1043 *Campylobacter jejuni* and thermotolerant *Campylobacter fetus* subsp *fetus*. JAMA.  
1044 1986;255: 361–364.

1045 90. Aureli P, Fenicia L, Pasolini B, Gianfranceschi M, McCroskey LM, Hatheway CL. Two  
1046 cases of type E infant botulism caused by neurotoxigenic *Clostridium butyricum* in Italy. J  
1047 Infect Dis. 1986;154: 207–211.

1048 91. Rood JI, Cole ST. Molecular genetics and pathogenesis of *Clostridium perfringens*.  
1049 Microbiol Rev. 1991;55: 621–648.

1050 92. Png CW, Lindén SK, Gilshenan KS, Zoetendal EG, McSweeney CS, Sly LI, et al.  
1051 Mucolytic bacteria with increased prevalence in IBD mucosa augment in vitro utilization of  
1052 mucin by other bacteria. Am J Gastroenterol. 2010;105: 2420–2428.

1053 93. Bergström A, Skov TH, Bahl MI, Roager HM, Christensen LB, Ejlerskov KT, et al.  
1054 Establishment of intestinal microbiota during early life: a longitudinal, explorative study of  
1055 a large cohort of Danish infants. Appl Environ Microbiol. 2014;80: 2889–2900.

1056 94. Le Doare K, Holder B, Bassett A, Pannaraj PS. Mother's milk: a purposeful contribution to  
1057 the development of the infant microbiota and immunity. Front Immunol. 2018;9: 361.

1058 95. Yassour M, Vatanen T, Siljander H, Hämäläinen A-M, Härkönen T, Ryhänen SJ, et al.  
1059 Natural history of the infant gut microbiome and impact of antibiotic treatment on bacterial  
1060 strain diversity and stability. Sci Transl Med. 2016;8: 343ra81.

1061 96. Pham VT, Lacroix C, Braegger CP, Chassard C. Early colonization of functional groups of  
1062 microbes in the infant gut. Environ Microbiol. 2016;18: 2246–2258.

1063 97. Vaishampayan PA, Kuehl JV, Froula JL, Morgan JL, Ochman H, Francino MP.  
1064 Comparative metagenomics and population dynamics of the gut microbiota in mother and  
1065 infant. Genome Biol Evol. 2010;2: 53–66.

1066 98. Marcabal A, Sonnenburg JL. Human milk oligosaccharide consumption by intestinal  
1067 microbiota. Clin Microbiol Infect. 2012;18: 12–15.

1068 99. Yatsunenko T, Rey FE, Manary MJ, Trehan I, Dominguez-Bello MG, Contreras M, et al.  
1069 Human gut microbiome viewed across age and geography. Nature. 2012;486: 222–227.

1070 100. Favier CF, Vaughan EE, De Vos WM, Akkermans ADL. Molecular monitoring of  
1071 succession of bacterial communities in human neonates. Applied and Environmental  
1072 Microbiology. 2002. pp. 219–226.

1073 101. Inoue R, Ushida K. Vertical and horizontal transmission of intestinal commensal bacteria  
1074 in the rat model. FEMS Microbiol Ecol. 2003;46: 213–219.

1075 102. Hopkins MJ, Macfarlane GT, Furrie E, Fite A, Macfarlane S. Characterisation of

1076        intestinal bacteria in infant stools using real-time PCR and northern hybridisation analyses.  
1077        FEMS Microbiol Ecol. 2005;54: 77–85.

1078        103. Urashima T, Odaka G, Asakuma S, Uemura Y, Goto K, Senda A, et al. Chemical  
1079        characterization of oligosaccharides in chimpanzee, bonobo, gorilla, orangutan, and  
1080        siamang milk or colostrum. Glycobiology. 2009;19: 499–508.

1081        104. Urashima T, Asakuma S, Leo F, Fukuda K, Messer M, Oftedal OT. The predominance of  
1082        type I oligosaccharides is a feature specific to human breast milk. Adv Nutr. 2012;3: 473S–  
1083        82S.

1084        105. Tao N, Wu S, Kim J, An HJ, Hinde K, Power ML, et al. Evolutionary glycomics:  
1085        characterization of milk oligosaccharides in primates. J Proteome Res. 2011;10: 1548–1557.

1086        106. Louis P, Flint HJ. Formation of propionate and butyrate by the human colonic  
1087        microbiota. Environ Microbiol. 2017;19: 29–41.

1088        107. Burger-van Paassen N, Vincent A, Puiman PJ, van der Sluis M, Bouma J, Boehm G, et  
1089        al. The regulation of intestinal mucin MUC2 expression by short-chain fatty acids:  
1090        implications for epithelial protection. Biochem J. 2009;420: 211–219.

1091        108. Rivera-Chávez F, Zhang LF, Faber F, Lopez CA, Byndloss MX, Olsan EE, et al.  
1092        Depletion of butyrate-producing *Clostridia* from the gut microbiota drives an aerobic  
1093        luminal expansion of *Salmonella*. Cell Host Microbe. 2016;19: 443–454.

1094        109. Chang PV, Hao L, Offermanns S, Medzhitov R. The microbial metabolite butyrate  
1095        regulates intestinal macrophage function via histone deacetylase inhibition. PNAS.  
1096        2014;111: 2247–2252.

1097        110. Millard AL, Mertes PM, Ittelet D, Villard F, Jeannesson P, Bernard J. Butyrate affects  
1098        differentiation, maturation and function of human monocyte-derived dendritic cells and  
1099        macrophages. Clin Exp Immunol. 2002;130: 245–255.

1100        111. Rokhsafat S, Lin A, Comelli EM. Mucin-microbiota interaction during postnatal  
1101        maturation of the intestinal ecosystem: clinical implications. Dig Dis Sci. 2016;61: 1473–  
1102        1486.

1103        112. Vatanen T, Kostic AD, d’Hennezel E, Siljander H, Franzosa EA, Yassour M, et al.  
1104        Variation in microbiome LPS immunogenicity contributes to autoimmunity in humans.  
1105        Cell. 2016;165: 1551.

1106        113. Laforest-Lapointe I, Arrieta M-C. Patterns of early-life gut microbial colonization during  
1107        human immune development: an ecological perspective. Front Immunol. 2017;8: 788.

1108        114. Mazmanian SK, Liu CH, Tzianabos AO, Kasper DL. An immunomodulatory molecule of  
1109        symbiotic bacteria directs maturation of the host immune system. Cell. 2005;122: 107–118.

1110        115. Round JL, Mazmanian SK. Inducible Foxp3+ regulatory T-cell development by a

1111        commensal bacterium of the intestinal microbiota. PNAS. 2010;107: 12204–12209.

1112    116. Telesford KM, Yan W, Ochoa-Reparaz J, Pant A, Kircher C, Christy MA, et al. A  
1113        commensal symbiotic factor derived from *Bacteroides fragilis* promotes human  
1114        CD39+Foxp3+ T cells and Treg function. Gut Microbes. 2015;6: 234–242.

1115    117. Troy EB, Kasper DL. Beneficial effects of *Bacteroides fragilis* polysaccharides on the  
1116        immune system. Front Biosci. 2010;15: 25–34.

1117    118. Schwab C, Gänzle M. Lactic acid bacteria fermentation of human milk oligosaccharide  
1118        components, human milk oligosaccharides and galactooligosaccharides. FEMS Microbiol  
1119        Lett. 2011;315: 141–148.

1120    119. Ward RE, Niñonuevo M, Mills DA, Lebrilla CB, German JB. In vitro fermentation of  
1121        breast milk oligosaccharides by *Bifidobacterium infantis* and *Lactobacillus gasseri*. Appl  
1122        Environ Microbiol. 2006;72: 4497–4499.

1123    120. Tsuboi KK, Kwong LK, Neu J, Sunshine P. A proposed mechanism of normal intestinal  
1124        lactase decline in the postweaned mammal. Biochem Biophys Res Commun. 1981;101:  
1125        645–652.

1126    121. Korpela K. Diet, microbiota, and metabolic Health: trade-off between saccharolytic and  
1127        proteolytic fermentation. Annu Rev Food Sci Technol. 2018;9: 65–84.

1128    122. Ren T, Boutin S, Humphries MM, Dantzer B, Gorrell JC, Coltman DW, et al. Seasonal,  
1129        spatial, and maternal effects on gut microbiome in wild red squirrels. Microbiome. 2017;5:  
1130        163.

1131    123. Moeller AH, Foerster S, Wilson ML, Pusey AE, Hahn BH, Ochman H. Social behavior  
1132        shapes the chimpanzee pan-microbiome. Science Advances. 2016;2: e1500997.

1133    124. Grieneisen L, Dasari M, Gould TJ, Björk JR, Grenier J-C, Yotova V, et al. Gut  
1134        microbiome heritability is nearly universal but environmentally contingent. Science.  
1135        2021;373: 181–186.

1136    125. Tung J, Barreiro LB, Burns MB, Grenier JC, Lynch J, Grieneisen LE, et al. Social  
1137        networks predict gut microbiome composition in wild baboons. eLife. 2015; e05224.

1138    126. Blekhman R, Tang K, Archie EA, Barreiro LB, Johnson ZP, Wilson ME, et al. Common  
1139        methods for fecal sample storage in field studies yield consistent signatures of individual  
1140        identity in microbiome sequencing data. Sci Rep. 2016;6: 1–5.

1141    127. Albers PCH, de Vries H. Elo-rating as a tool in the sequential estimation of dominance  
1142        strengths. Anim Behav. 2001;61: 489–495.

1143    128. Neumann C, Duboscq J, Dubuc C, Ginting A, Irwan AM, Agil M, et al. Assessing  
1144        dominance hierarchies: validation and advantages of progressive evaluation with Elo-rating.  
1145        Anim Behav. 2011;82: 911–921.

1146 129. Puff C, Nemomissa S. Plants of the Simen: a flora of the Simen Mountains and  
1147 surroundings, northern Ethiopia. National Botanic Garden (Belgium); 2005.

1148 130. Tinsley Johnson E, Snyder-Mackler N, Lu A, Bergman TJ, Beehner JC. Social and  
1149 ecological drivers of reproductive seasonality in geladas. *Behav Ecol.* 2018;29: 574–588.

1150 131. Gohl DM, Vangay P, Garbe J, MacLean A, Hauge A, Becker A, et al. Systematic  
1151 improvement of amplicon marker gene methods for increased accuracy in microbiome  
1152 studies. *Nat Biotechnol.* 2016;34: 942–949.

1153 132. Bolyen E, Rideout JR, Dillon MR, Bokulich NA, Abnet CC, Al-Ghalith GA, et al.  
1154 Reproducible, interactive, scalable and extensible microbiome data science using QIIME 2.  
1155 *Nat Biotechnol.* 2019;37: 852–857.

1156 133. Callahan BJ, McMurdie PJ, Rosen MJ, Han AW, Johnson AJA, Holmes SP. DADA2:  
1157 High-resolution sample inference from Illumina amplicon data. *Nat Methods.* 2016;13:  
1158 581–583.

1159 134. Quast C, Pruesse E, Yilmaz P, Gerken J, Schweer T, Yarza P, et al. The SILVA  
1160 ribosomal RNA gene database project: improved data processing and web-based tools.  
1161 *Nucleic Acids Res.* 2013;41: D590–6.

1162 135. Team RC. R: A language and environment for statistical computing. Vienna; 2015.

1163 136. Bisanz JE. qiime2R: Importing QIIME2 artifacts and associated data into R sessions.  
1164 Version 0.99. 2018;13.

1165 137. McMurdie PJ, Holmes S. phyloseq: an R package for reproducible interactive analysis  
1166 and graphics of microbiome census data. *PLoS One.* 2013;8: e61217.

1167 138. Kembel SW, Cowan PD, Helmus MR, Cornwell WK, Morlon H, Ackerly DD, et al.  
1168 Picante: R tools for integrating phylogenies and ecology. *Bioinformatics.* 2010;26: 1463–  
1169 1464.

1170 139. Wood SN. Stable and efficient multiple smoothing parameter estimation for Generalized  
1171 Additive Models. *J Am Stat Assoc.* 2004;99: 673–686.

1172 140. McMurdie PJ, Holmes S. Waste not, want not: why rarefying microbiome data is  
1173 inadmissible. *PLoS Comput Biol.* 2014;10: e1003531.

1174 141. Arnhold E. easynls: Easy nonlinear model. R Package Version 5.0, 1–9. 2017.

1175 142. Aitchison J. The Statistical Analysis of Compositional Data. *J R Stat Soc Series B Stat*  
1176 *Methodol.* 1982;44: 139–160.

1177 143. Palarea-Albaladejo J, Martín-Fernández JA. zCompositions – R package for multivariate  
1178 imputation of left-censored data under a compositional approach. *Chemometrics and*  
1179 *Intelligent Laboratory Systems.* 2015. pp. 85–96.

1180 144. Gloor GB, Macklaim JM, Pawlowsky-Glahn V, Egoscue JJ. Microbiome datasets are  
1181 compositional: and this is not optional. *Front Microbiol.* 2017;8: 2224.

1182 145. Oksanen J, Blanchet FG, Kindt R, Legendre P, O'hara RB, Simpson GL, et al. Vegan:  
1183 community ecology package. R package version 1.17-4. URL <http://CRAN.R-project.org/package=vegan>. 2010; 1–5.

1185 146. Wilmanski T, Diener C, Rappaport N, Patwardhan S, Wiedrick J, Lapidus J, et al. Gut  
1186 microbiome pattern reflects healthy ageing and predicts survival in humans. *Nature Metabolism.* 2021;3: 274–286.

1188 147. Márquez EJ, Chung C-H, Marches R, Rossi RJ, Nehar-Belaid D, Eroglu A, et al. Sexual-  
1189 dimorphism in human immune system aging. *Nat Commun.* 2020;11: 1–17.

1190 148. Zeileis A, Grothendieck G. *zoo: S3 infrastructure for regular and irregular time series.*  
1191 *Journal of Statistical Software.* 2005.

1192 149. Hyndman RJ, Khandakar Y. Automatic time series forecasting: the forecast package for  
1193 R. *Journal of Statistical Software.* 2008;27: 1–22.

1194 150. Tiessen A, Cubedo-Ruiz EA, Winkler R. Improved representation of biological  
1195 information by using correlation as distance function for heatmap cluster analysis. *Am J  
1196 Plant Sci.* 2017;08: 502–516.

1197 151. Syakur MA, Khotimah BK, Rochman EMS, Satoto BD. Integration K-means clustering  
1198 method and Elbow method for identification of the best customer profile cluster. *IOP Conf  
1199 Ser: Mater Sci Eng.* 2018;336: 012017.

1200 152. Zhao S, Guo Y, Sheng Q, Shyr Y. Heatmap3: an improved heatmap package with more  
1201 powerful and convenient features. *BMC Bioinformatics.* 2014;15: P16.

1202

1203

1204

## 1205 **Figure 1. Gut microbiome taxonomic assembly in the first three years of life in immature** 1206 **geladas.**

1207 (A, B) Taxonomic composition of the immature gelada gut microbiome at the phylum and family  
1208 level as a function of age. The relative abundance of each taxon was calculated per sample by  
1209 dividing the counts of the taxa by sequencing depth, and then averaged across samples belonging  
1210 to the age category of interest. Age was split into categories for visualization purposes, but analyses  
1211 treated age as a continuous variable. (C) Age-associated pattern of alpha diversity within samples,  
1212 as calculated by the Shannon index (richness and evenness of Amplicon Sequencing Variants,  
1213 ASVs). The vertical line represents the critical point of inflexion (calculated using quadratic  
1214 plateau models) representing the age at which alpha diversity converges to adult-like patterns. The  
1215 dataset was rarefied at 20,000 reads for the figure. (D,E) Age-associated pattern of beta diversity.  
1216 A Principal Component Analysis (PCA) was used to ordinate the samples based on the Aitchison  
1217 dissimilarity index (which is simply the Euclidean distance after centered-log-ratio transformation  
1218 of the raw counts). Panel D represents the projection of the first principal component (PC1) that is  
1219 best explained by the age of immatures. The vertical line represents the critical point of inflexion  
1220 (calculated using quadratic plateau models) representing the age at which beta diversity converges  
1221 to adult-like patterns. Panel E shows how age structures the gut microbiome composition of  
1222 immatures on the two first principal components. (F) Comparison of gut microbiome composition  
1223 between mother and offspring, as assessed using 398 matched mother-infant pairs of fecal samples  
1224 collected on the same day. Here, the number of shared ASVs between pairs of samples is  
1225 represented. The vertical line represents the critical point of inflexion (calculated using quadratic

1226 plateau models) representing the age at which the number of shared ASVs stabilizes to its maximal  
1227 value. The dataset was rarefied at 20,000 reads for the calculation. (G) Age distribution inter-  
1228 individual variability in gut microbiomes using the ASV-level unweighted and weighted UniFrac  
1229 distances. This score was calculated as the minimum pairwise dissimilarity value from a beta  
1230 diversity matrix for a given immature sample, and captures how dissimilar a sample is from its  
1231 nearest neighbor, given all other gut microbiome samples in the immature cohort. Higher values  
1232 indicate a more distinct gut microbiome from the population. The dataset was rarefied at 20,000  
1233 reads for the calculation.

1234

1235 **Figure 2. Age-associated changes in microbial composition at the family level.**

1236 (A) Heatmap of the microbial families exhibiting a significant chronological trend as a function of  
1237 age (fitted values from ARIMA models and predicted using LOESS regression per taxa as a  
1238 function of age). Values represent z-score normalized counts after centered-log-ratio (clr)  
1239 transformation. Hierarchical clustering was used to group age-dependent trajectories into four  
1240 clusters exhibiting similar chronological trends. Color bars on the left side identify the clusters.  
1241 Taxa (i.e. rows) are ordinated on the heatmap using correlation as distance function. All microbial  
1242 families above 0.01% abundance were analyzed (N=55) and the 53 that displayed a significant  
1243 trend are represented. (B) Relative abundance of 8 functionally important microbial families that  
1244 are enriched in early life (belonging to cluster 1), as a function of age. The age-dependent  
1245 trajectories were calculated on clr-transformed counts, but here for interpretation purposes we  
1246 represent the LOESS regression on the raw relative abundance across samples (same for panels C  
1247 and D). (C) Relative abundance of 5 functionally important microbial families that peak in  
1248 abundance around 10 months of age (belonging to cluster 2). Relative abundance is represented

1249 on a log-scale to accommodate high and low abundance families together. (D) Relative abundance  
1250 of 8 functionally important microbial families that are enriched in later life (belonging to cluster  
1251 4). Relative abundance is represented on a log-scale to accommodate high and low abundance  
1252 families together.

1253

1254 **Figure 3. Composition of the early-life microbiota at the genus level.**

1255 Relative abundance of functionally important genera in early life, as a function of age. The age-  
1256 dependent trajectories were calculated on clr-transformed counts. For visualization purposes  
1257 however, we represent the LOESS regression on the raw relative abundance across samples (on a  
1258 log-transformed scale).

1259

1260 **Figure 4. Age-associated changes in the functional profile of the gut microbiome of**  
1261 **immatures based on predicted KEGG orthologs (KO) metagenomes.**

1262 (A) Relative abundance of metabolic pathways (left: KO level 2 and right: KO level 3 of the  
1263 carbohydrate metabolism) enriched in early life, as a function of age. (B) Relative abundance of  
1264 metabolic pathways (KO level 3) that peak in abundance or decrease in abundance at 10 months  
1265 of age. (C) Relative abundance of metabolic pathways (at KO level 2) enriched in later life, as a  
1266 function of age. In all plots, the average curve is the LOESS regression on the raw relative  
1267 abundance across samples.

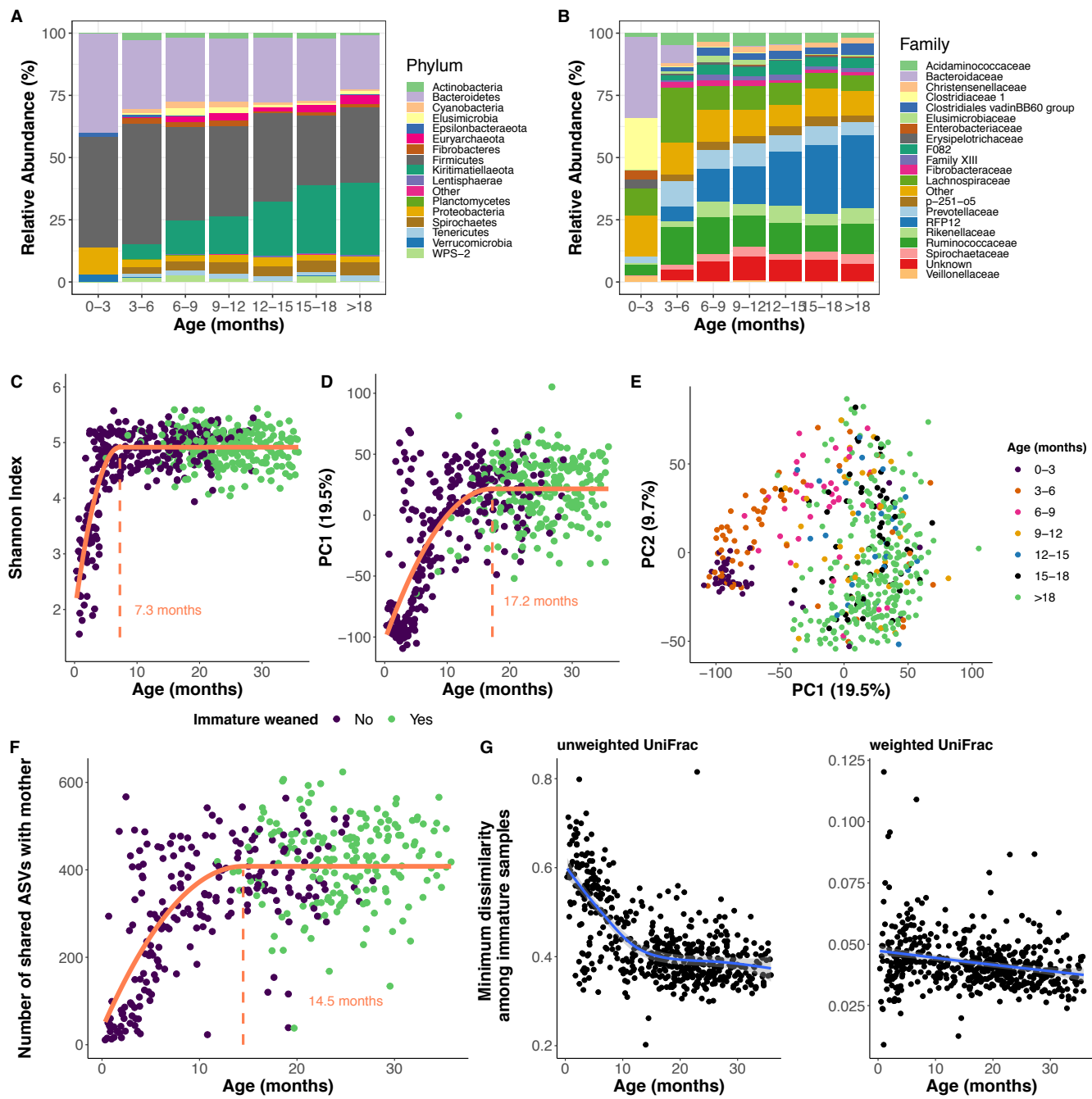
1268

1269 **Figure 5. The effect of maternal parity on offspring's gut microbiota functional capacity.**

1270 (A) Metabolic pathways (KO level 2 for upper row and KO level 3 for lower row) that are more  
1271 abundant in infants <12 months) born to primiparous females than infants of multiparous females.

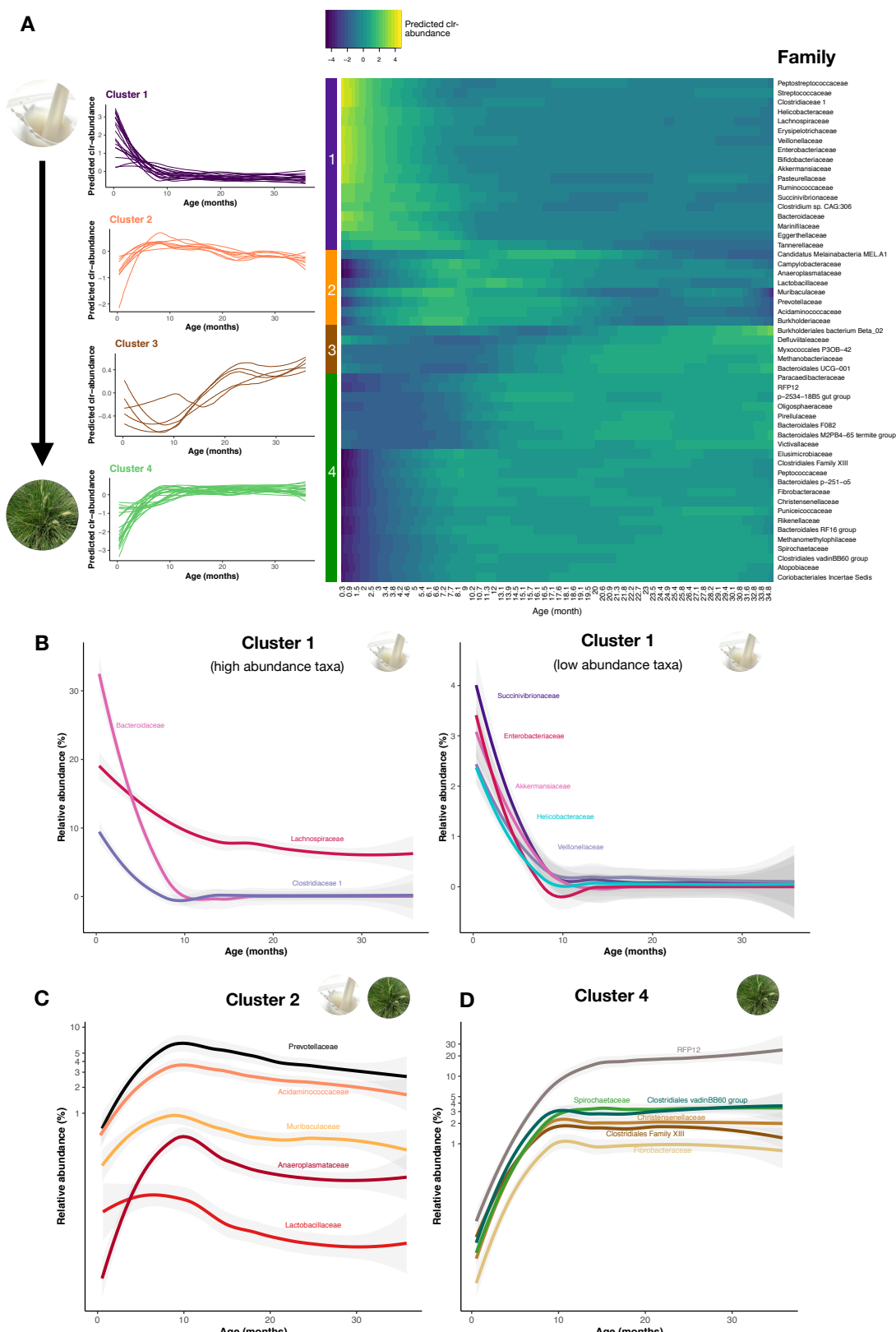
1272 (B) Metabolic pathways (KO level 2) that are less abundant in infants (<12 months) born to  
1273 primiparous females than infants of multiparous females. (C) Results of the nonparametric  
1274 resampling approach testing if offspring share more Amplicon Sequencing Variants (ASVs) and  
1275 have a more similar gut microbiome composition (unweighted UniFrac dissimilarity) to their  
1276 mother than to random adult females of the population. The histograms show the random  
1277 distribution of the metric of interest (i.e. when matching each infant sample to a random female  
1278 sample collected during the same season, with 1000 repetitions). The vertical line shows the  
1279 observed value of the metric (i.e. between the actual mother-offspring pairs of fecal samples  
1280 collected the same day). This analysis was performed separately on young (nursing) infants (aged  
1281 0-12 months, N=136 samples) and old immatures (>18 months, N=201) that were likely weaned.  
1282 (D) Composition of the shared ASVs between young infants (<12 months) and their mothers. The  
1283 ASVs that are commonly shared between mother-offspring pairs (e.g. among > 70% of the pairs)  
1284 in early life tend to have high loading scores of the first principal component (PC1) of a Principal  
1285 Component Analysis ordination (based on Aitchison distance). Since PC1 strongly correlates  
1286 positively with age, these shared ASVs are characteristic of later life. (E) Vertical transmission  
1287 differs for primiparous and multiparous females in early life. Young infants (<12 months) born to  
1288 primiparous females share fewer ASVs with their mother and have a more dissimilar gut  
1289 microbiome composition (unweighted UniFrac dissimilarity) compared to their mother than  
1290 offspring born to multiparous females. Later in life (>18 months), immatures born to primiparous  
1291 and multiparous females are equally similar to their mother in terms of gut microbiome  
1292 composition.

1293 **Figure 1.**

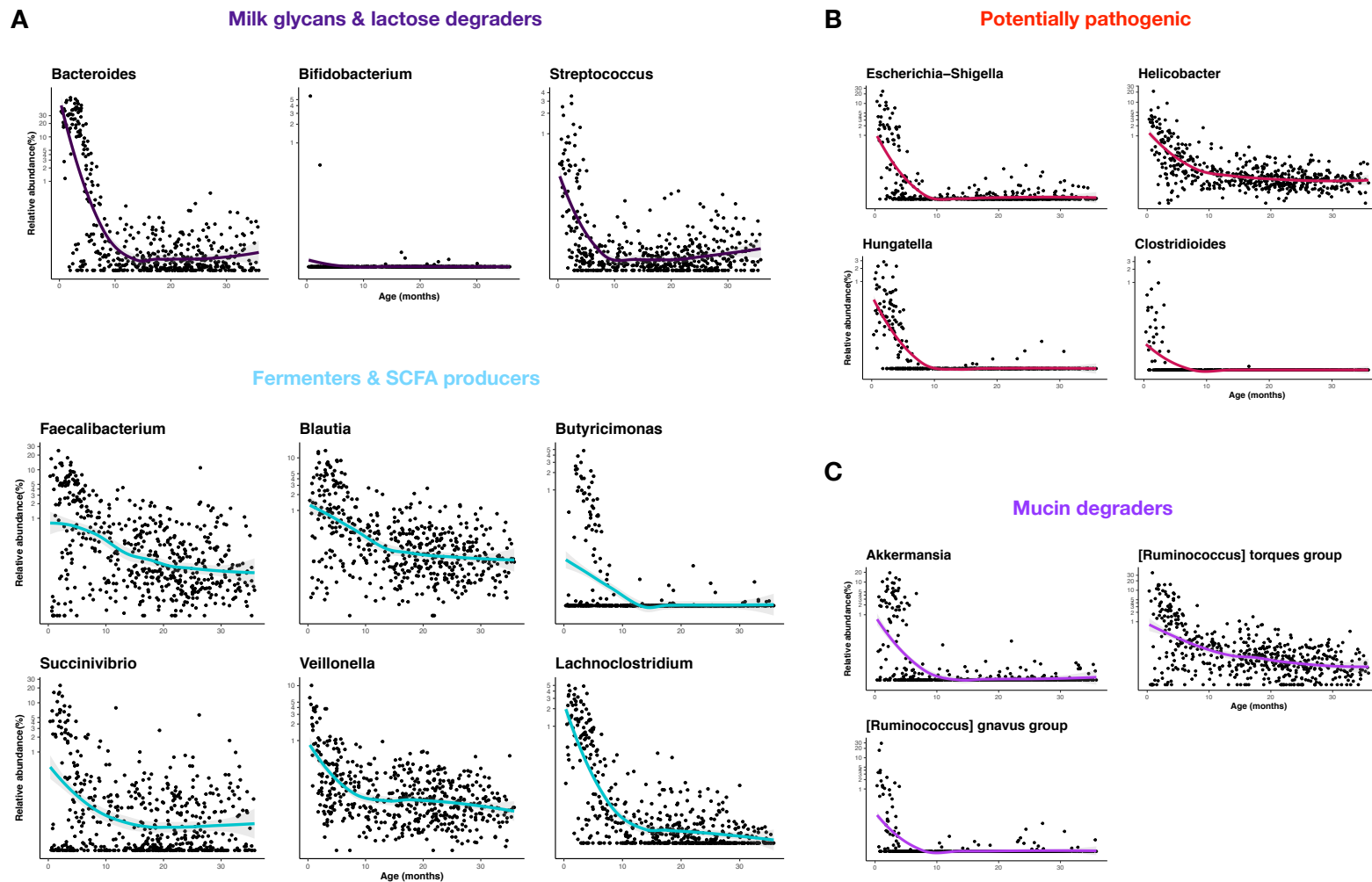


1294

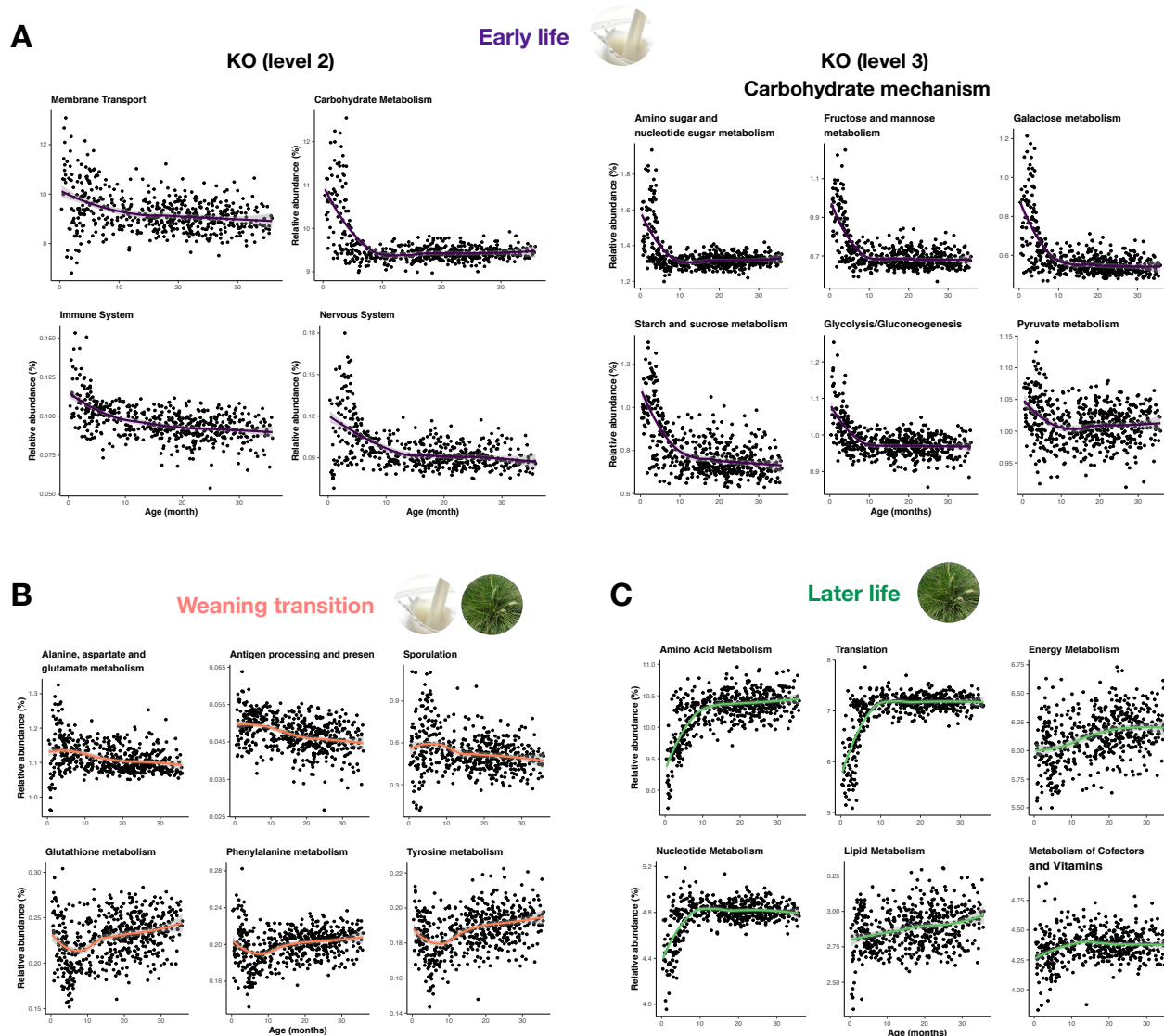
1295 **Figure 2.**



1297 **Figure 3.**



1299 **Figure 4.**



1301 **Figure 5.**

